Frontiers of Instrumentation in Nuclear Science

Paul O'Connor

Brookhaven National Laboratory

Instrumentation Division

Frontiers of Instrumentation in Nuclear Science

Paul O'Connor

Brookhaven National Laboratory

Instrumentation Division

- **BNL Introduction and History**
- **Detectors: Smaller, Faster, Quieter**
- **Systems: Larger, Denser, Colder**

Outline

- **BNL Instrumentation Division**
  - Facilities, accomplishments
- **Detector and Electronics Trends (with selected examples)**
  - Improved time resolution
    - Silicon detectors with avalanche gain
    - Wideband electronics
  - Improved spatial resolution
    - Fine-pitch pixels
    - Interpolation techniques
  - Improved energy resolution
    - Si detectors with low collection capacitance
    - Monolithic integration of sensors and electronics
    - Repetitive non-destructive readout
    - Cryogenic devices
- **Highly-scaled systems**
  - Inhospitable environments
    - Cryo
    - Vacuum
    - Radiation
  - Power and data bandwidth constraints

Outline

- **BNL Instrumentation Division**
  - **Facilities, accomplishments**

- **Detector and Electronics Trends (with selected examples)**
  - **Improved time resolution**
    - **Silicon detectors with avalanche gain**
    - **Wideband electronics**
  - **Improved spatial resolution**
    - **Fine-pitch pixels**
    - **Interpolation techniques**
  - **Improved energy resolution**
    - **Si detectors with low collection capacitance**
    - **Monolithic integration of sensors and electronics**
    - **Repetitive non-destructive readout**
    - **Cryogenic devices**

- **Highly-scaled systems**
  - **Inhospitable environments**
    - **Cryo**
    - **Vacuum**
    - **Radiation**
  - **Power and data bandwidth constraints**

BNL Instrumentation Division

Mission
- Develop state-of-the-art instrumentation for current and future Laboratory programs
- Technology transfer

Established
1948

Division Head
Dr. David M. Asner

Staff
•16 Scientific
•3 Post Doctoral
•8 Professional
•13 Technical
•4 Administrative

Research Areas
•Semiconductor detectors
•Gas and Noble liquid detectors
•Microelectronics
•Lasers and Optics
•Micro/Nano fabrication

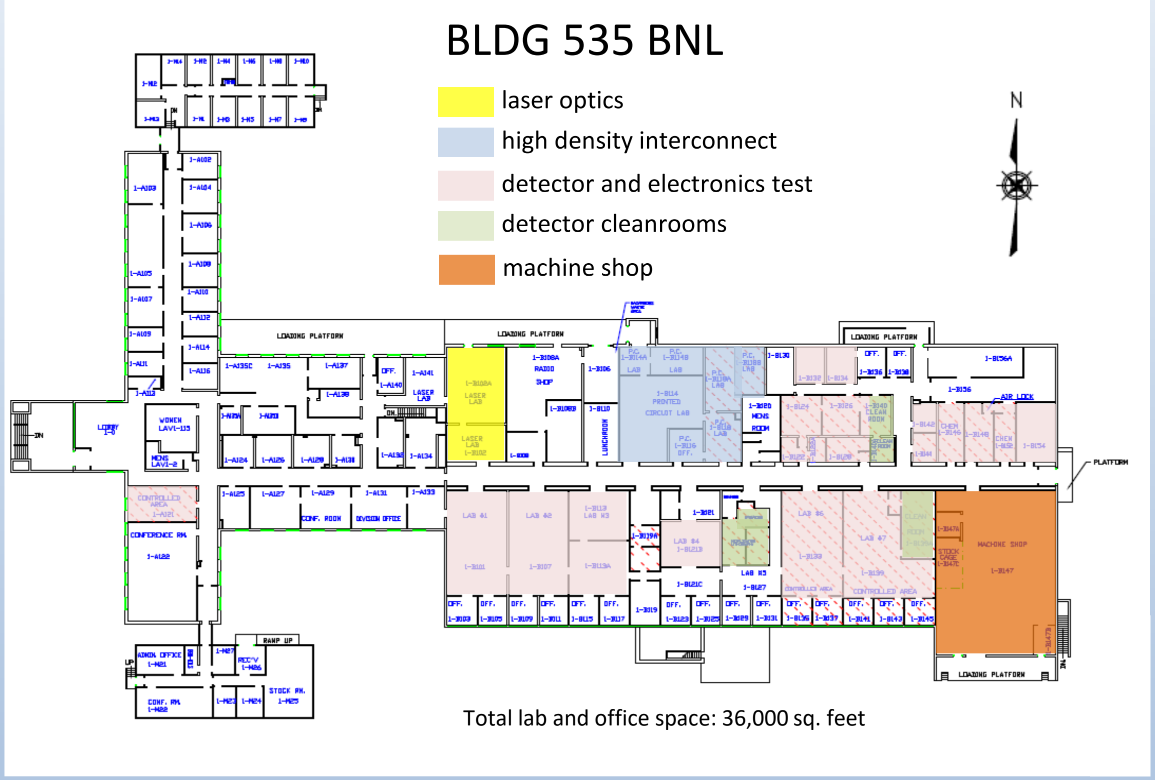

Highlights of Accomplishments – first 35 years

- Gas detectors, electronics - (1948)
- Fast(μs) transistorized electronics for physics experiments - (1956)
- First Si detectors, nanosecond electronics - (1960)
- Positron emission tomography detector - (1960)
- Germanium detectors, low noise electronics - (1965)
- LAr ionization chambers for calorimetry - (1973)
- Detectors for neutron scattering - (1976)
- Optical metrology - (1979)
- Electron microscopy, MEMS - (1980)
- First synchrotron X-ray detectors - (1982)
- Silicon Drift Detector (1983)

Preamp optimal filtering1983

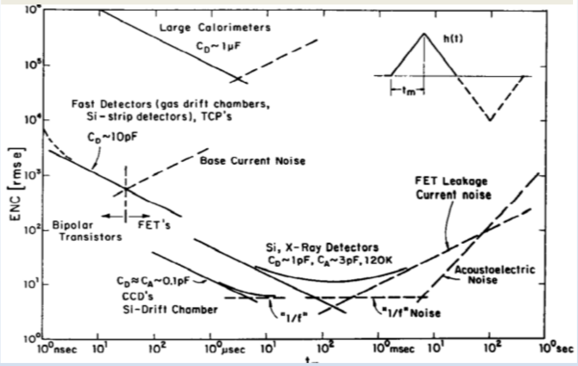

Spark Chambers in Muon Neutrino Discovery
Lederman, Schwartz, Steinberger,1962, Nobel Prize 1988

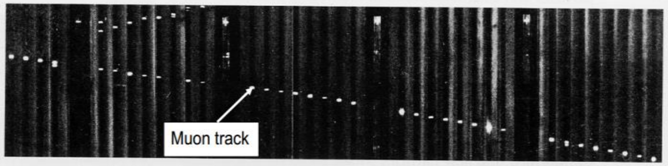

Solar Neutrinos at Homestake Mine
Davis 1967-1985, Nobel Prize 2002

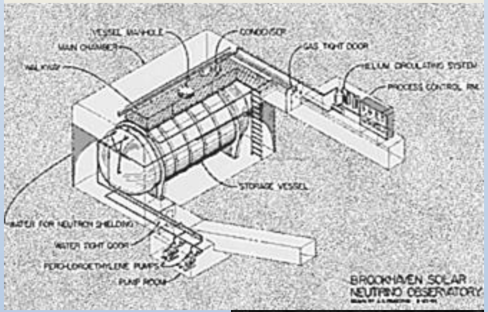

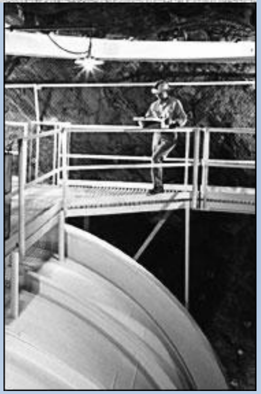

Silicon drift detector 1983

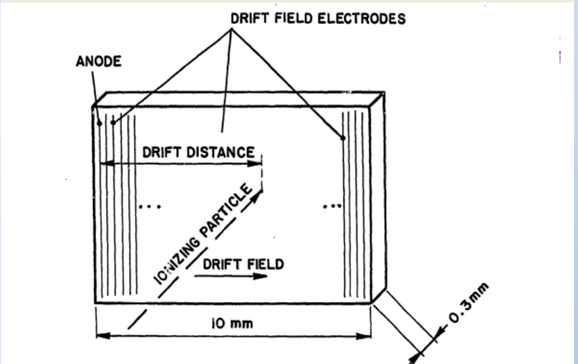

Fig. 8. Silicon Drift Chamber. The wafer is about .3 mm thick and has a front area of few cm^2. The surface is covered by a strip array of p^+ junction electrodes which provides the depletion and the drift field. (Only junctions at the extremes of the wafer are shown.) Electrons produced by the passage of a fast charged particle drift toward the anode which is the only readout channel on the wafer.

Germanium Detector Breakthrough 1963

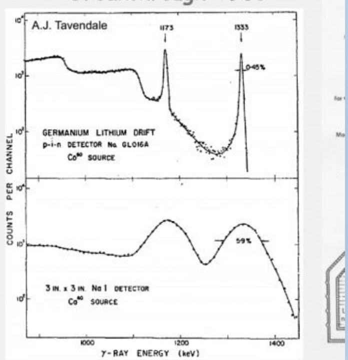

BNL charge preamp with JFET at ~120K, 1968

Bubble chamber: charmed baryon decay 1975

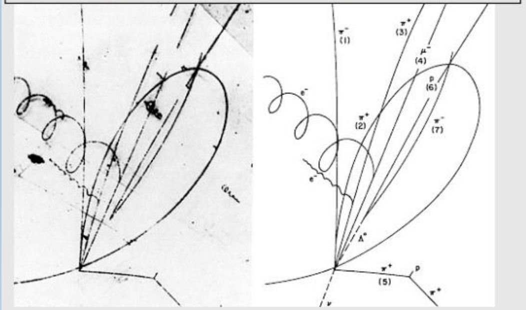

Positron Emission Tomograph 1960

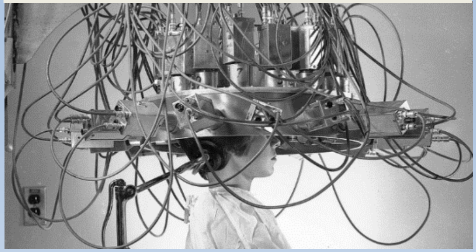

Highlights of Accomplishments – first 35 years

- Gas detectors, electronics - (1948)
- Fast(µs) transistorized electronics for physics experiments - (1956)
- First Si detectors, nanosecond electronics - (1960)
- Positron emission tomography detector - (1960)
- Germanium detectors, low noise electronics - (1965)
- LAr ionization chambers for calorimetry - (1973)
- Detectors for neutron scattering - (1976)
- Optical metrology - (1979)
- Electron microscopy, MEMS - (1980)
- First synchrotron X-ray detectors - (1982)
- Silicon Drift Detector (1983)

Preamp optimal filtering1983

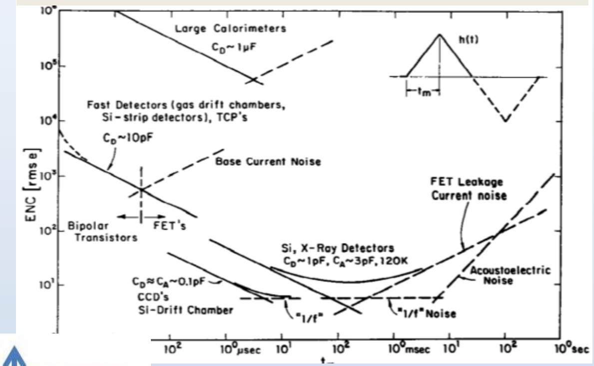

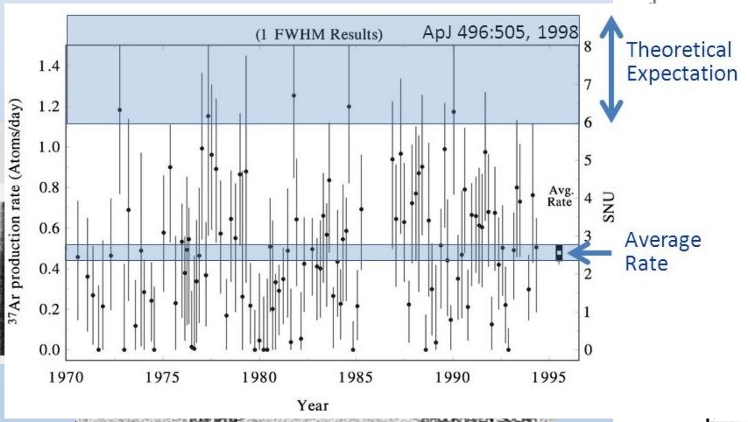

icon drift detector 1983

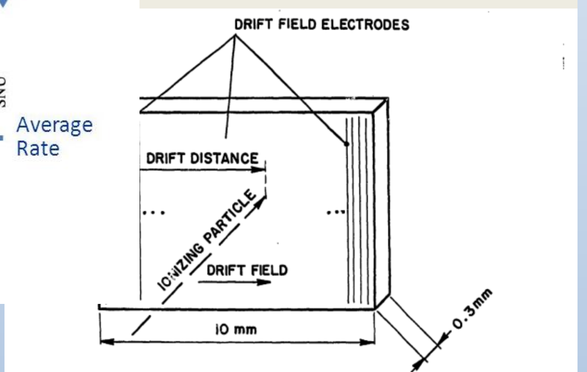

Fig. 8. Silicon Drift Chamber. The wafer is about .3 mm thick and has a front area of few cm². The surface is covered by a strip array of p⁺ junction electrodes which provides the depletion and the drift field. (Only junctions at the extremes of the wafer are shown.) Electrons produced by the passage of a fast charged particle drift toward the anode which is the only readout channel on the wafer.

Leder... ze 1988

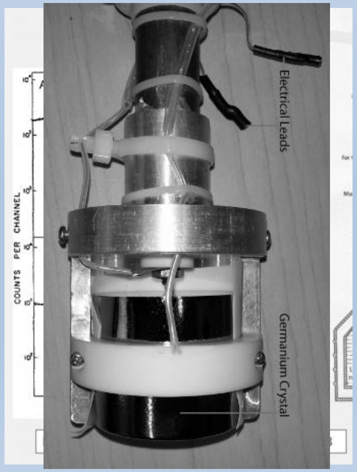

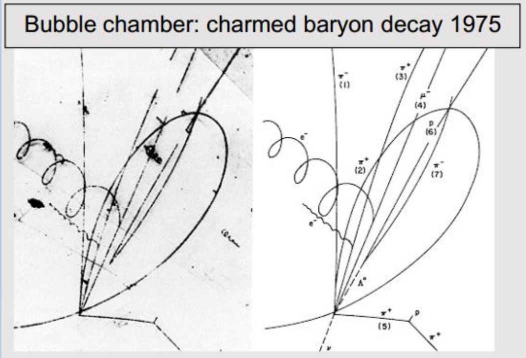

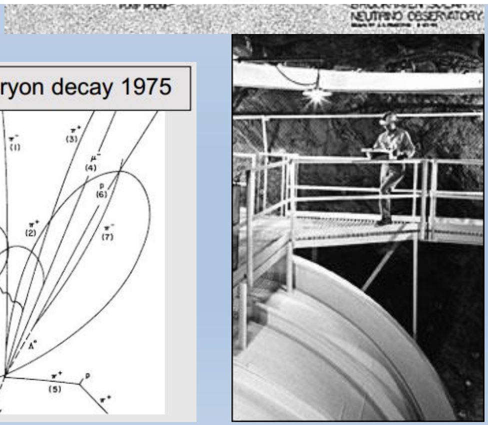

Positron Emission Tomograph 1960

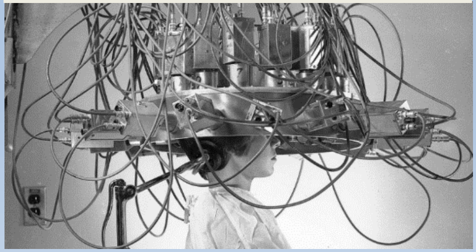

Highlights of Accomplishments – past 35 years

- Cryogenic electronics - (1984)
- Lasers in accelerator technology - (1985)
- Si detectors for HEP/NP - (1986)
- Gas detectors for heavy ion physics - (1986)
- Long Trace Profiler - (1987)
- Monolithic low-noise circuits - (1990)
- LAr, LKr ionization chambers, SSC, LHC: - (1993)
- Nanostructures - (1994)
- Deep sub-micron low-noise circuits - (1997)
- Ultrafast optical techniques - (2000)
- Neutron/Gamma detectors for Homeland Security - (2002)
- Small animal imaging - (2003)
- Silicon detectors for synchrotron radiation - (2004)
- Fully-depleted CCD arrays and readout for astronomy - (2005)
- Beam diagnostics - (2006)
- Diamond detectors – (2009)
- LAr Time Projection Chambers - (2009)
- Low Temperature Microelectronics - (2010)

cold CMOS electronics

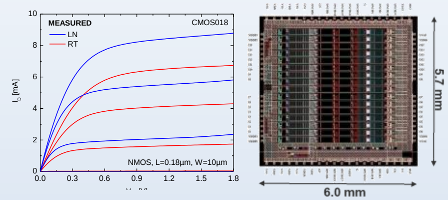

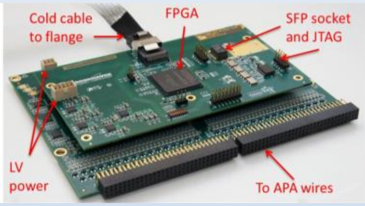

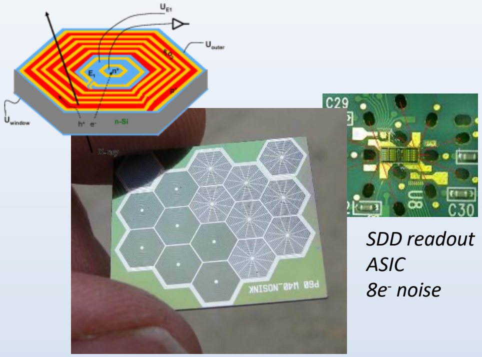

high resolution hexagonal SDD array

SDD readout ASIC 8e^- noise

384-element EXAFS array HERMES/SCEPTER readout

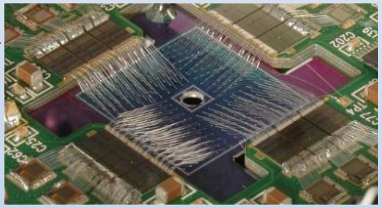

LSST focal plane

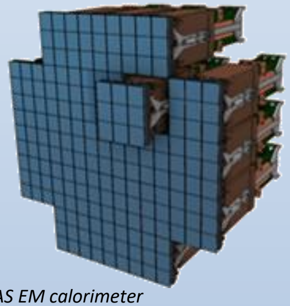

LSST raft tower module

120° thermal neutron detector

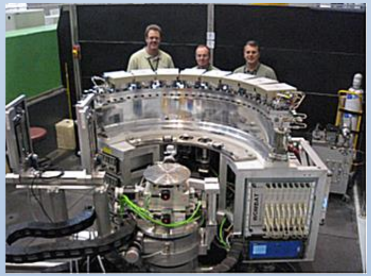

PHENIX Time Expansion Chamber/TRD

Compact Gamma Camera

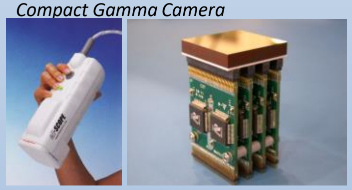

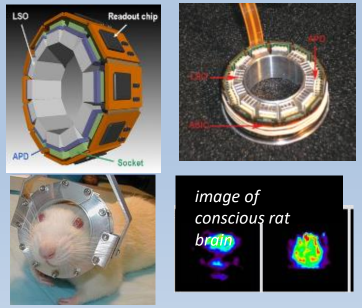

240-channel multichp module

ATLAS EM calorimeter

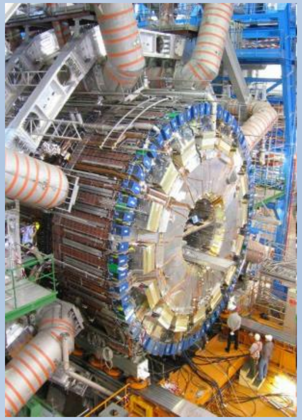

70-ton LAr TPC (MICROBOONE)

Diamond detector for x-ray beam position monitor

Outline

- BNL Instrumentation Division
  - Facilities, accomplishments
- **Detector and Electronics Trends (with selected examples)**
  - **Improved time resolution**
    - **Silicon detectors with avalanche gain**
    - **Wideband electronics**
  - Improved spatial resolution
    - Fine-pitch pixels
    - Interpolation techniques
  - Improved energy resolution
    - Si detectors with low collection capacitance
    - Monolithic integration of sensors and electronics
    - Repetitive non-destructive readout
    - Cryogenic devices
- Highly-scaled systems
  - Inhospitable environments
    - Cryo
    - Vacuum
    - Radiation
  - Power and data bandwidth constraints

Time resolution/rate capability

Detecting the time of occurrence of an ionizing event involves a chain of events, each of which has a duration with statistical fluctuations:

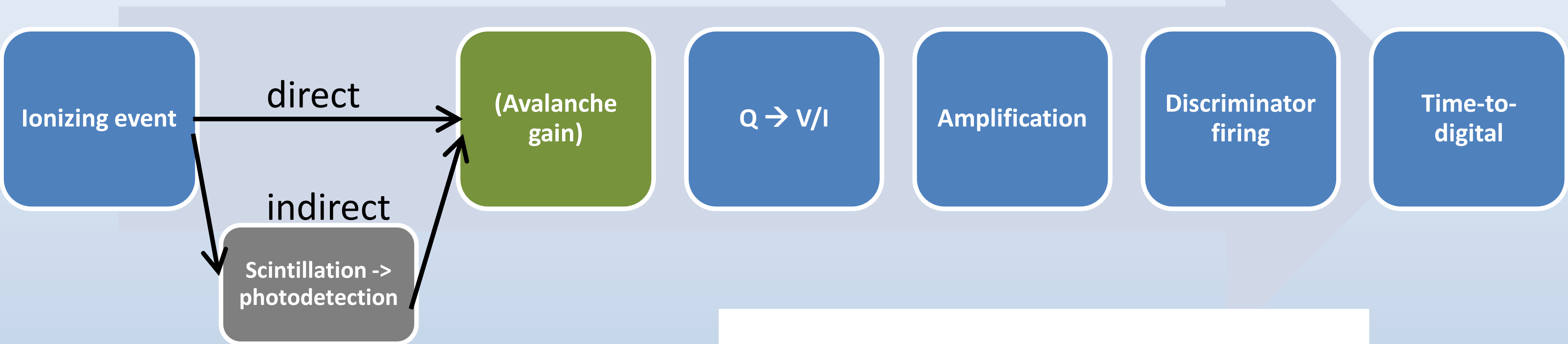

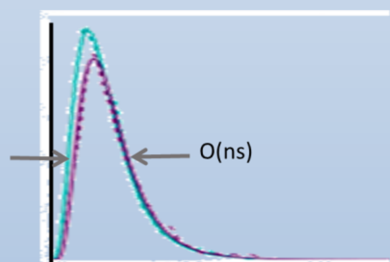

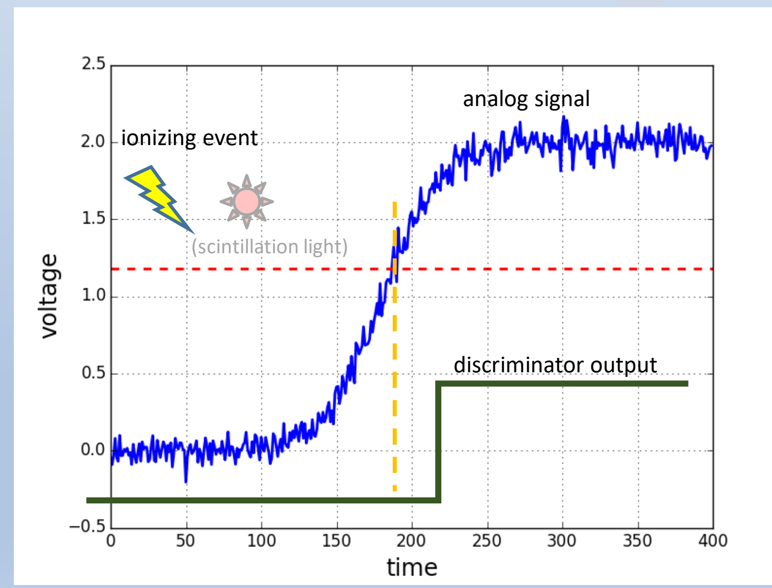

Contributions to timing resolution

- Ionization: prompt (< 1ps)
- Transport of ionization charge
- If using scintillator: generation and transport of scintillation photons; photon statistics noise
- Amplifier noise – see below
- TDC quantization noise ~binsize/sqrt(12)

Electronics noise/speed tradeoff (white noise)

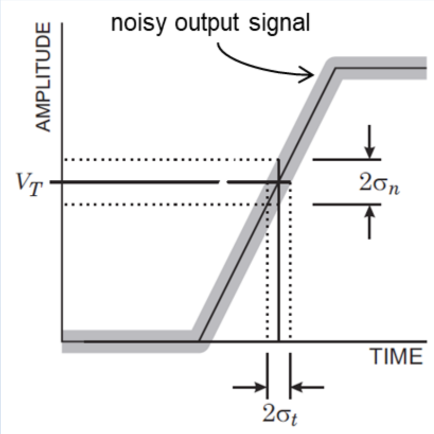

$$\sigma_T = \frac{\sigma_Q}{\left(\frac{dv_0}{dt}\right)}$$

➔ time resolution improves as the slope of the waveform at the threshold crossing increases

Slope at z.c. $\frac{dv_0}{dt} \sim \frac{V_0}{t_{rise}} \sim \frac{V_0}{\sqrt{t_{amp}^2 + t_{signal}^2}}$

for white series noise $\sigma_Q \sim t_{amp}^{-\frac{1}{2}}$

$$\sigma_T = \frac{\sigma_Q}{\frac{dv_0}{dt}} \sim \frac{\frac{1}{V_0}\sqrt{t_{amp}^2 + t_{signal}^2}}{\sqrt{t_{amp}}} = \frac{\sqrt{t_{signal}}}{V_0}\sqrt{\frac{t_{amp}}{t_{signal}} + \frac{t_{signal}}{t_{amp}}}$$

minimum when $\boldsymbol{t_{amp} = t_{signal}}$

Solid-state detectors with internal multiplication

APD ("Avalanche PhotoDiode")

- Direct ionization charge is drifted to a high-field region where avalanche multiplication takes place.
- (Linear) multiplication factor M depends on reverse bias; typically M ~ 20-200.
- Avalanche mechanism has statistical fluctuation → excess noise, but at low signal level overall S/N is improved because input-referred electronics noise is reduced by M.
- Custom fabrication process

SPAD ("single photon avalanche diode")

- an APD operated in breakdown, with quenching mechanism to allow fast recovery. Single ehp can be amplified to mA current level. Loss of linear response but fast. Custom fabrication process

SiPM ("silicon photomultiplier")

- an array of $\mathcal{O}(10^3)$ SPADs connected in parallel to a common output. Analog output is analog sum of charge pulses ~ number of photons.

Digital SiPM

- array of SPADs with embedded electronics; arranged to generate 2 digital outputs encoding (a) number of photons and (b) timestamp. Standard CMOS fabrication process.

Solid-state avalanche devices increasingly replacing vacuum photomultiplier tubes (PMT), which are bulky, fragile, expensive, and inoperable in magnetic fields.
Commercial sector push for automotive LIDAR, TOF-PET, optical communications.

Solid-state detectors with internal multiplication

APD

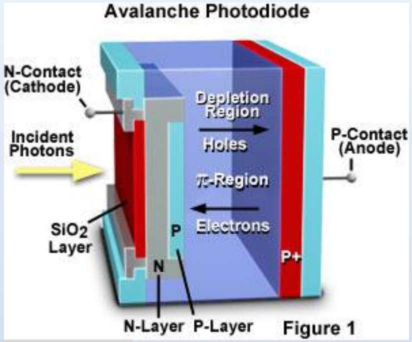

SPAD

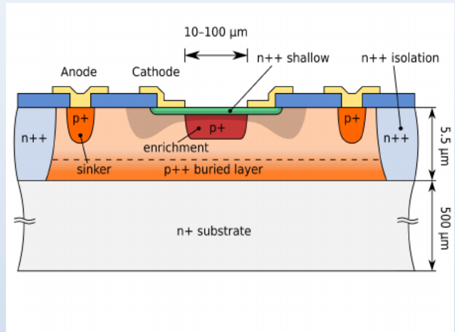

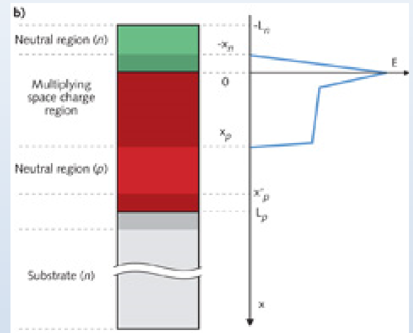

SPTR 24ps FWHM

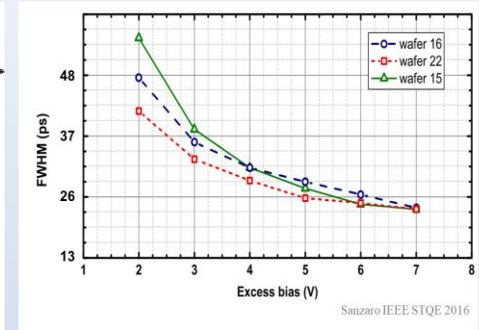

SiPM

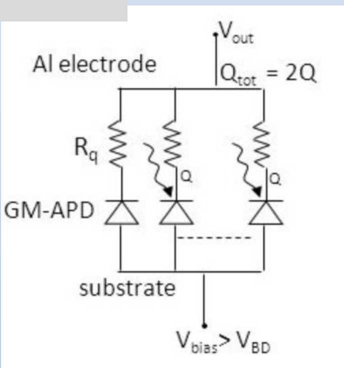

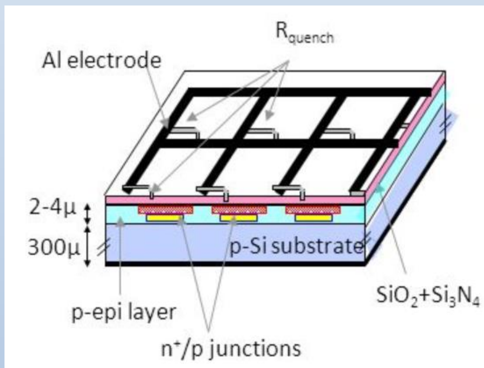

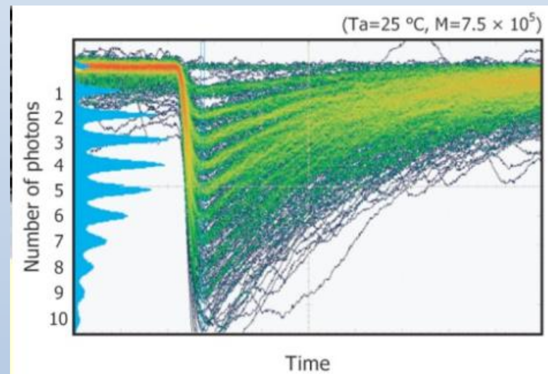

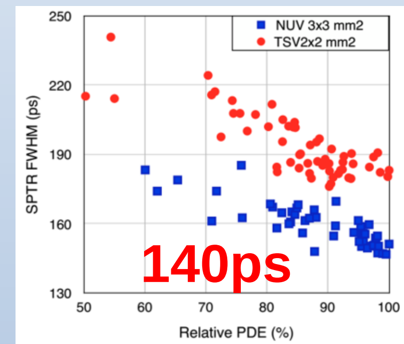

Nemallapudi *et al* 2016 *JINST* **11** P10016

Digital-SiPM

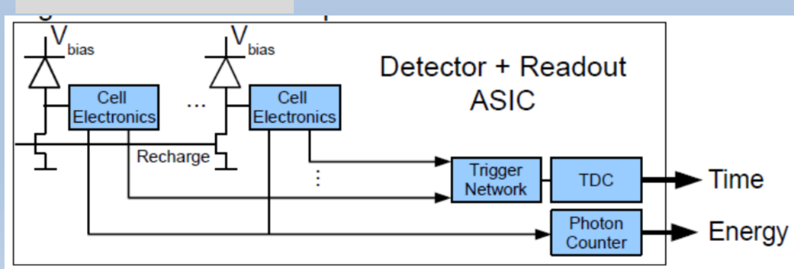

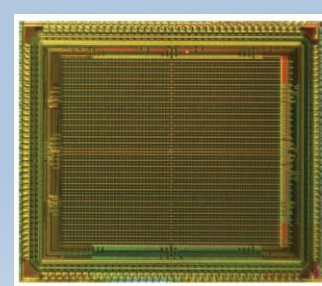

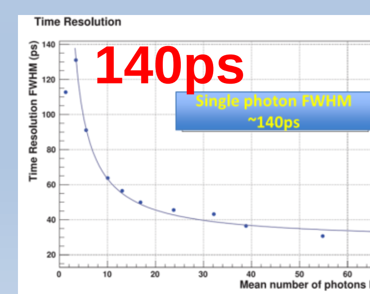

Frach 2009

Large-scale SiPM application in collider detectors

Near-term: sPHENIX calorimeter at BNL ~2020

- >120k used in calorimeter of sPHENIX (E. Mannel)

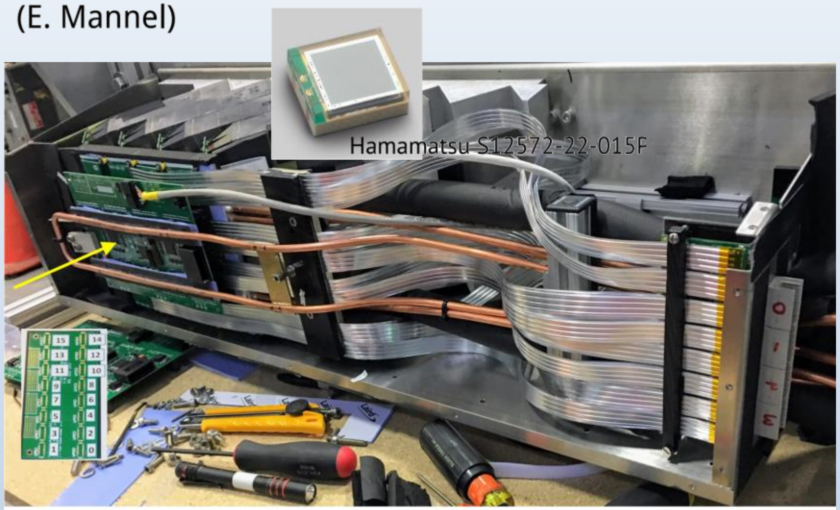

EMCal

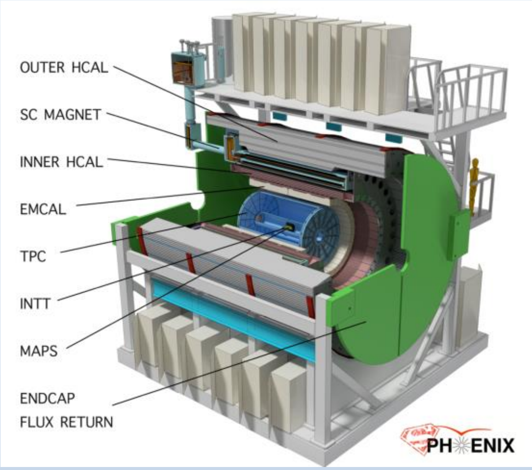

Longer-term:

CMS high-luminosity upgrade at LHC ~2024

MIP timing detector: thin scintillator + 250K chan SiPM

High granularity endcap hadronic calorimeter: 500m^2 plastic scintillator with SiPM on-tile readout

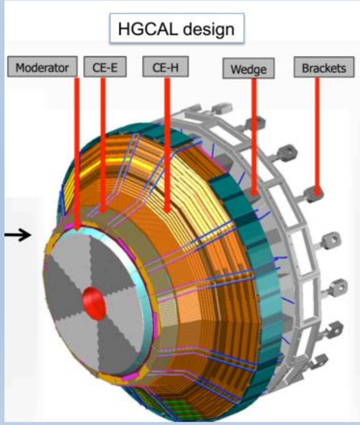

nEXO 5-ton l-^{136}Xe TPC $0\nu\beta\beta$

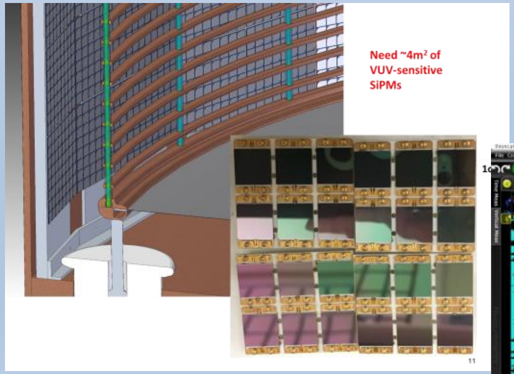

HPK VUV4

Test at BNL with pulsed 177nm light source

Low Gain Avalanche Photodiode (LGAD)

- APD engineered for fast (O(10ps)) timing.
- Target application: high granularity timing detector for determining longitudinal vertex position in HL-LHC.
- Also suitable for fast/high-rate photon detection.

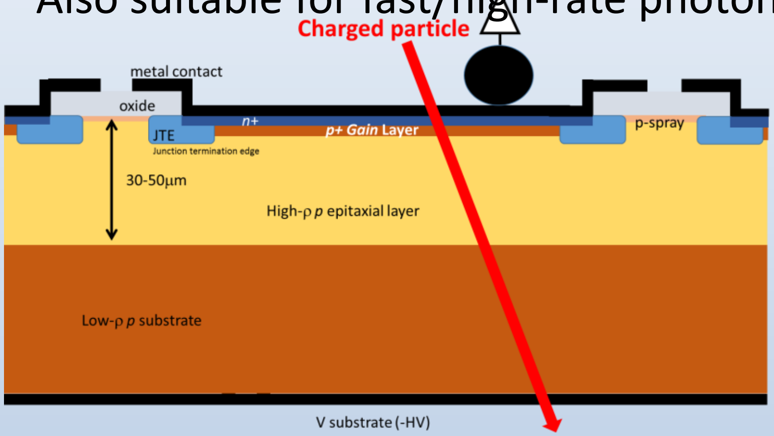

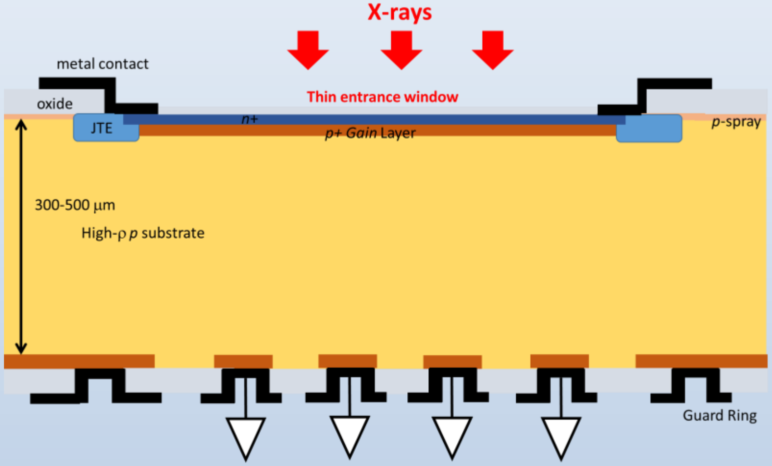

BNL technology demonstrated:

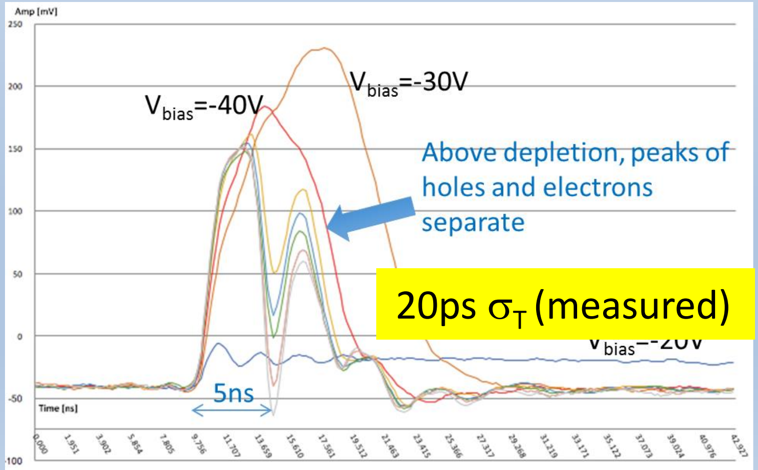

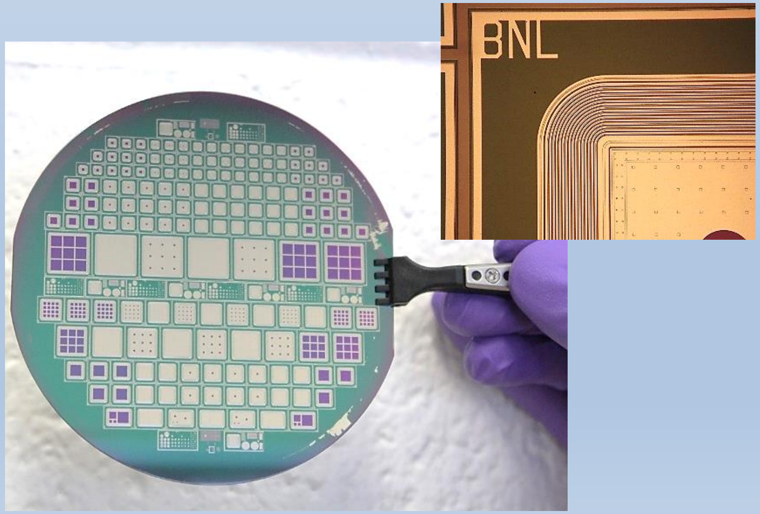

Giacomini 2018 pers. comm.

Threshold detection: noise rate

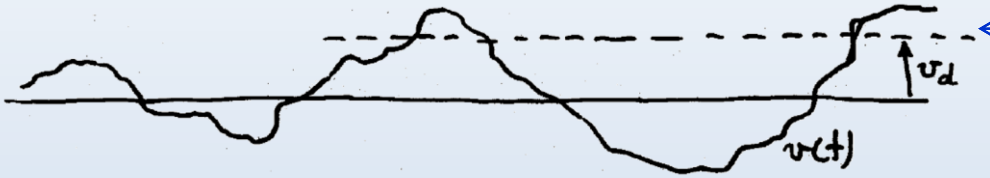

Equivalent noise rate:

$$\boldsymbol{ENR = f_0 \exp(-\frac{Q_T^2}{2Q_N^2})}$$

Q_T = threshold
Q_N = noise

f_0 = rate of positive zero crossings:

$$f_0 = \frac{1}{2\pi} * \left(-\frac{K'(0)}{K(0)}\right)^{\frac{1}{2}} = \frac{1}{2\pi}\left(\frac{\int_0^\infty \omega^2 W(\omega)d\omega}{\int_0^\infty W(\omega)d\omega}\right)^{\frac{1}{2}}$$

$\approx 1/2\pi T_p$

$W(\omega)$ = spectral density
$K(\tau)$ = autocorrelation function
$K(0)^{\frac{1}{2}} = Q_N$
T_P = pulse peaking time

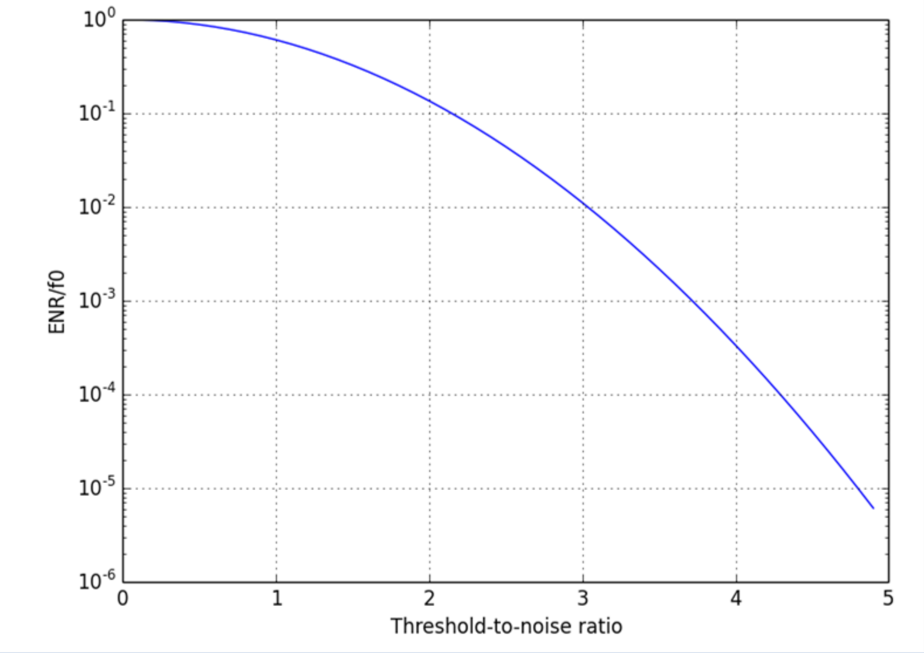

Threshold detection: example

Pulse peaking time	T_P = 500ns
Number of channels	N_{ch} = 100,000
Requirement	ENR < 1kHz

$$ENR = f_0 exp\left(-\frac{Q_T^2}{2Q_N^2}\right) < 10^3 Hz$$

$$f_0 \approx \frac{1}{2\pi T_p} = 318kHz \text{ per channel}$$ (white noise, semiGaussian shaper)

$$\frac{Q_T}{Q_N} > 2\sqrt{-\ln\left(\frac{10^3}{3.18 \cdot 10^5 \cdot 10^5}\right)}$$

$$\frac{Q_T}{Q_N} > \ 8.3$$

Low electronics noise more critical for detection limit in large-N_{ch} systems

Outline

- BNL Instrumentation Division
  - Facilities, accomplishments
- Detector and Electronics Trends (with selected examples)
  - Improved time resolution
    - Silicon detectors with avalanche gain
    - Wideband electronics
  - Improved spatial resolution
    - Fine-pitch pixels
    - Interpolation techniques
  - Improved energy resolution
    - Si detectors with low collection capacitance
    - Monolithic integration of sensors and electronics
    - Repetitive non-destructive readout
    - Cryogenic devices
- Highly-scaled systems
  - Inhospitable environments
    - Cryo
    - Vacuum
    - Radiation
  - Power and data bandwidth constraints

Energy-resolving detector family tree

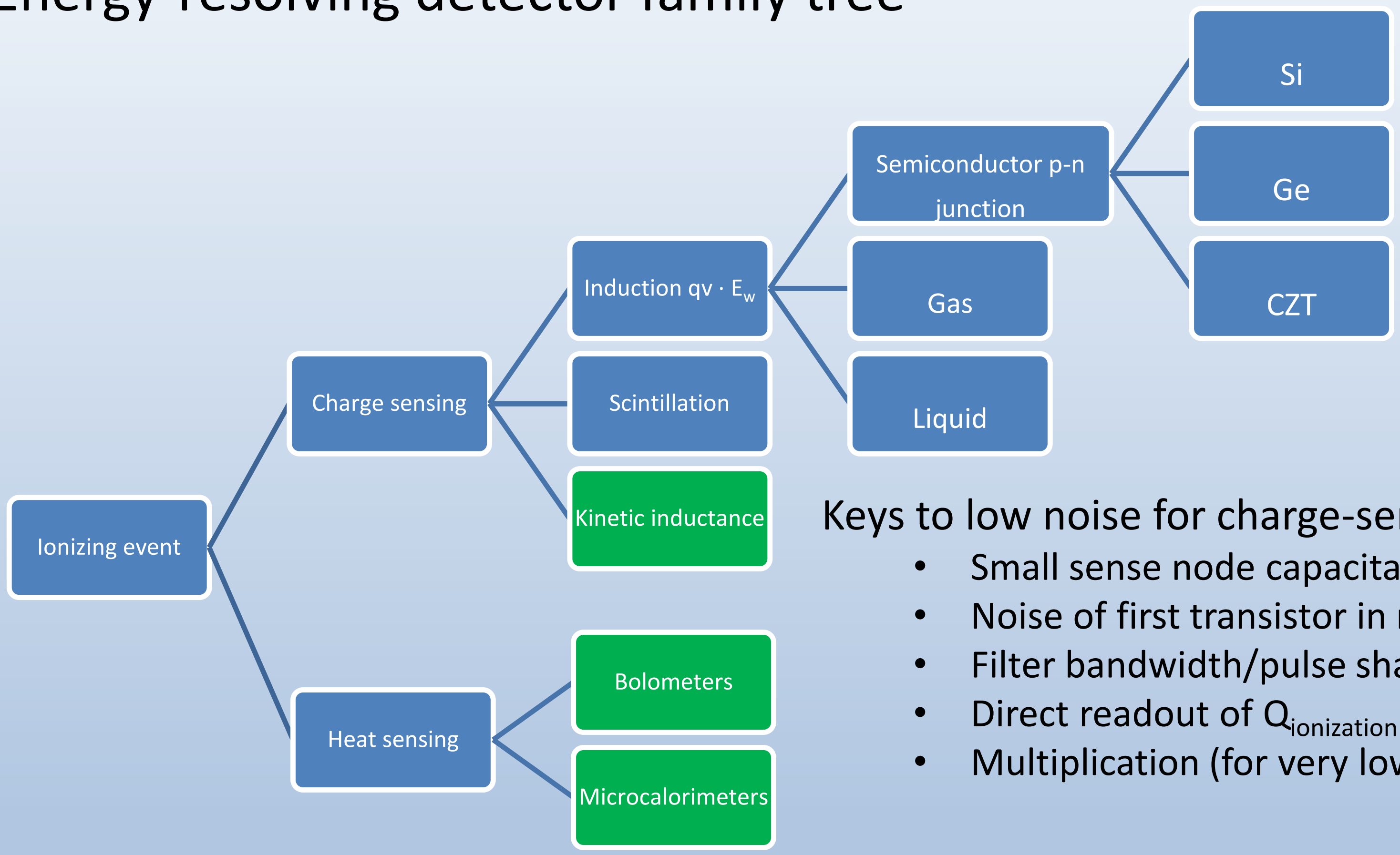

Keys to low noise for charge-sensing detectors:

- Small sense node capacitance C_{det}
- Noise of first transistor in readout chain
- Filter bandwidth/pulse shaping time
- Direct readout of $Q_{ionization}$ where possible
- Multiplication (for very low signals)

Si-based detectors

CCD Charge Coupled Device

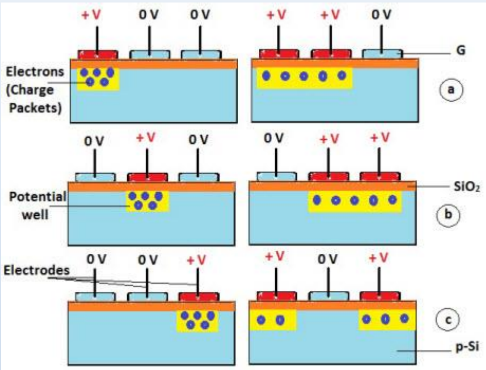

- Charge integrated in potential wells formed by polysilicon gates and implant boundaries
- After integration, gate potentials are sequenced to transfer charge to low-capacitance sense node and on-sensor amplifier
- Noise performance:
    - ~3e- at 100kpix/s
    - ~10e- at 1Mpix/s
- Custom fabrication process

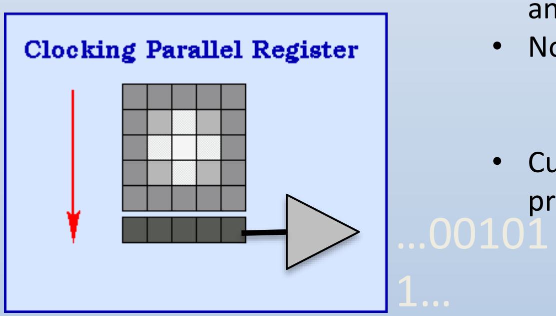

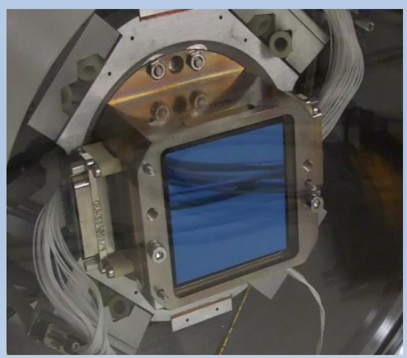

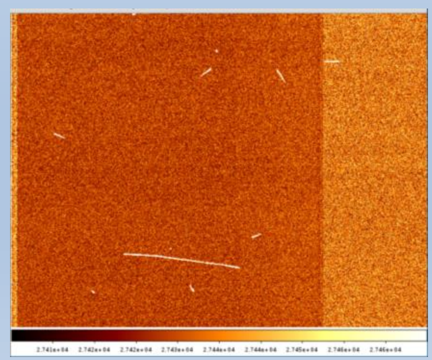

SDD Silicon Drift Detector

linear

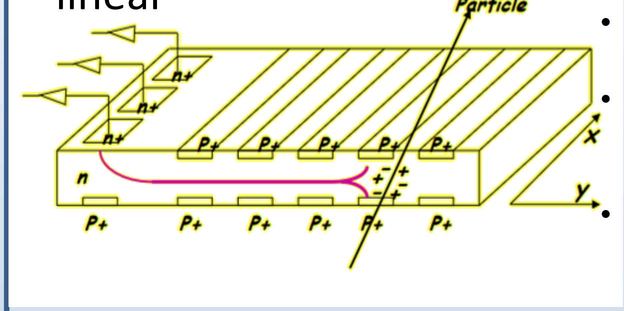

- Inbuilt depletion and drift fields.
- Potential minimum in center of wafer
- Anode capacitance small despite large sensitive area

radial

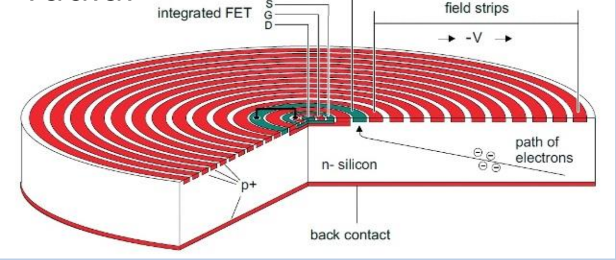

Noise vs. temp.

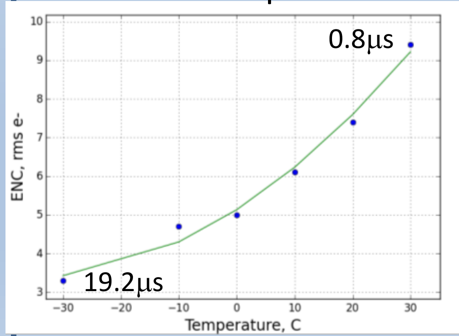

Bertuccio 2018 IEEE T-NS 2016(63)

STAR SVT @ BNL (2003)

Si-based detectors with integrated electronics

MAPS Monolithic Active Pixel Sensor

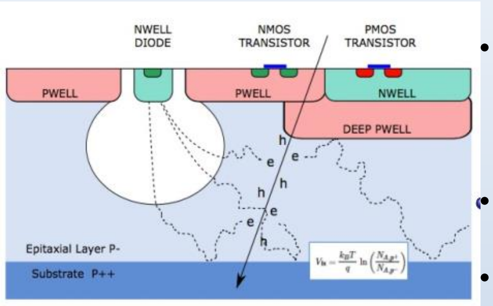

STAR HFT @ RHIC 2014 360Mpix

sPHENIX MVTX@ RHIC 2020 225Mpix HR-CMOS

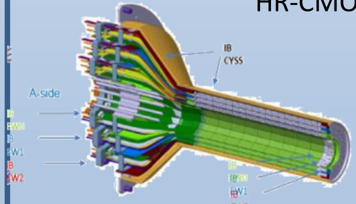

ALICE ITS @ LHC 2021

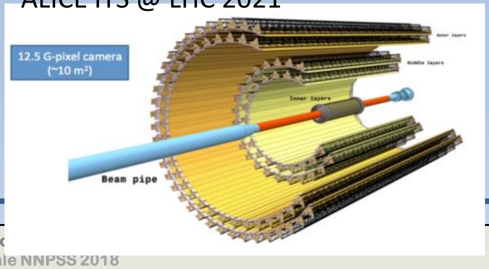

- Conventional CMOS fabrication process using shallow depleted bulk as photodiode.
- In-pixel amplification, reset, output switching.
- Sometimes, incorporate single-stage CCD in pixel for CDS noise reduction
- Arbitrary amount of CMOS circuitry outside sensing area
- Extensive use in commodity/consumer cameras
- Hope – to replace hybrid pixels for cost, compactness, lower power, lower material budget in trackers
- Challenges – small depletion thickness in standard CMOS process; radiation intolerance. HV-CMOS under intensive study

DEPFET Depleted Field Effect Transistor

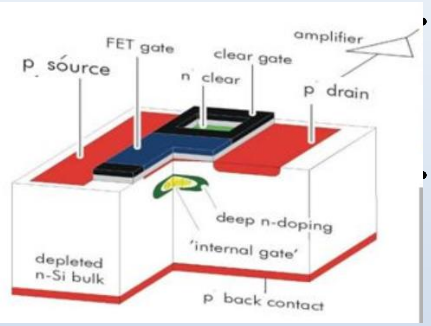

- Built-in potential minimum causes e- charge to be steered to the "back gate"/"internal gate" of a JFET transistor.
- Directly control JFET current, minimal capacitance.

Equivalent circuit

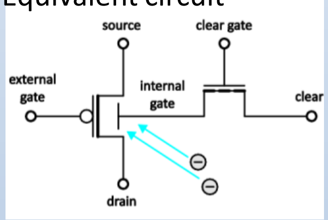

DEPFET array

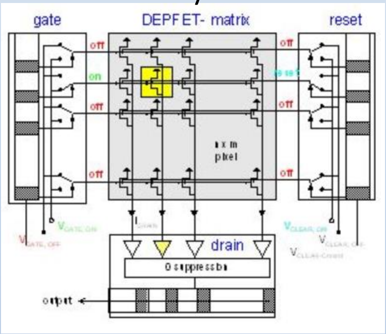

ATHENA WFI

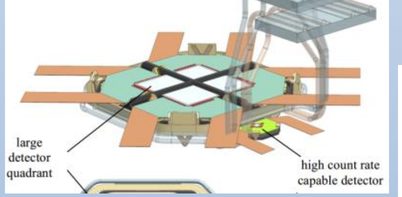

BELLE II PXD

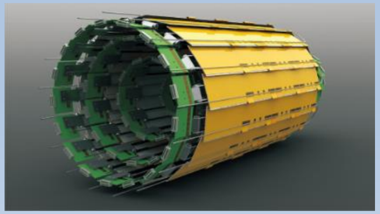

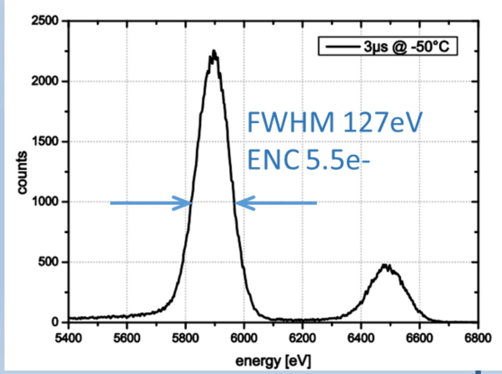

Aschauer *et al* 2017 *JINST* **12** P11013

Noise reduction by repetitive non-destructive readout (RNDR)

- RMS noise of a single measurement is typically determined by the electronic noise of the first amplifier transistor.
- In detectors where charge motion can be deterministically controlled (CCD, DEPFET) it is possible to introduce multiple, statistically independent measurements (N) of the same charge packet. White noise contribution from the front end electronics can be averaged down as √N (“Skipper”).
- Charge carrier lifetime at moderately reduced temperature (140K) is O(minutes) ➔ charge loss can be virtually excluded.
- “Skipper” CCDs and DEPFETs have recently demonstrated ***sub-0.2e-*** read noise and opened the possibility for sensitive measurements of low-mass neutral particle – nucleus interactions where extremely low thresholds are required. Particular interest focused on DM candidates in the MeV mass region, experimentally largely unexplored.

- DAMIC: low-noise standard CCD for low-mass Dark Matter search
- SENSEI: skipper CCD for low-mass Dark Matter search.
  - ***Has already established tightest constraints on DM cross section in the 0.5 – 4MeV mass range after only 0.019 gram-days surface run.***
- DANAE: skipper DEPFET for low-mass Dark Matter search
- CONNIE: low-noise standard CCD for Coherent Elastic Neutrino-Nucleus Scattering.

CCD and DEPFET results with RNDR

Skipper CCD

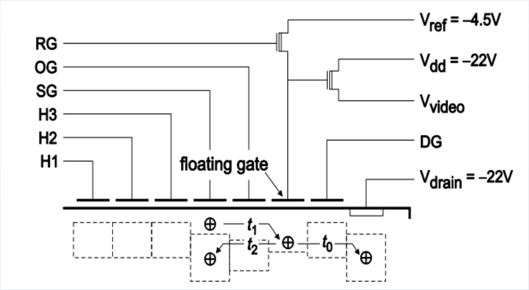

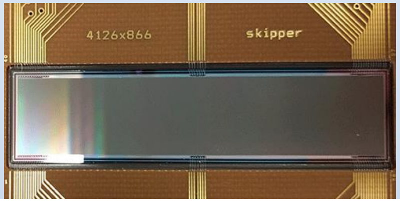

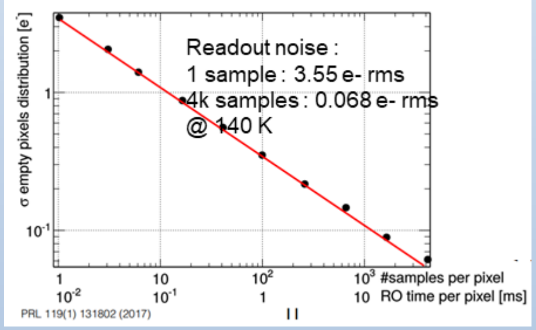

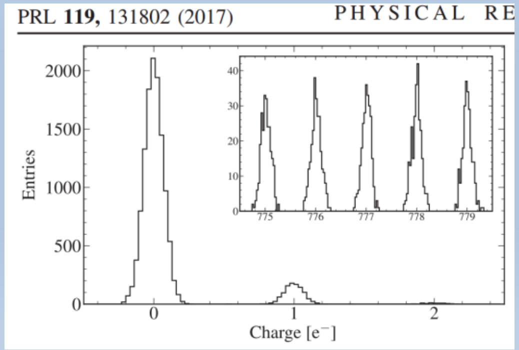

Skipper DEPFET

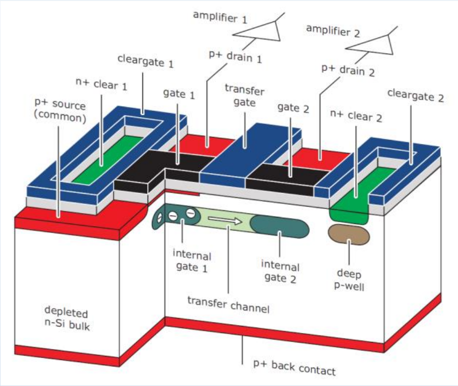

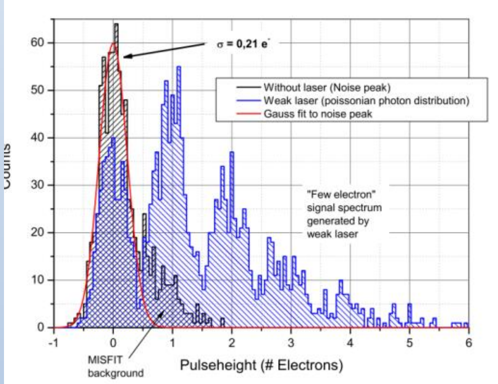

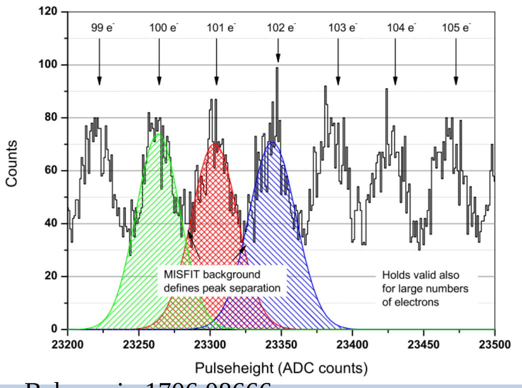

Bahr arxiv 1706.08666

Superconductor-based detectors

Microwave Kinetic Inductance Detecors (MKIDs)
Bolometers and microcalorimeters with Transition Edge Sensor thermometry (TES)
Require operating temperatures O(10^{-3}K)
Thermal, time, and frequency multiplexing techniques for minimizing cryostat penetrations

Ge detector (1963): 100X improvement over NaI scintillator at ~MeV

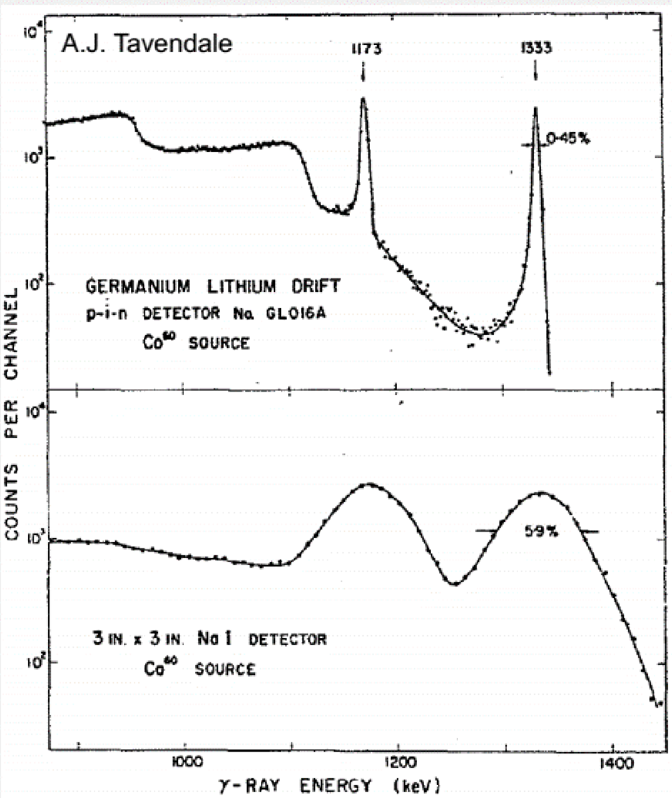

TES bolometer (2013): 100X improvement over Si(Li) at ~keV

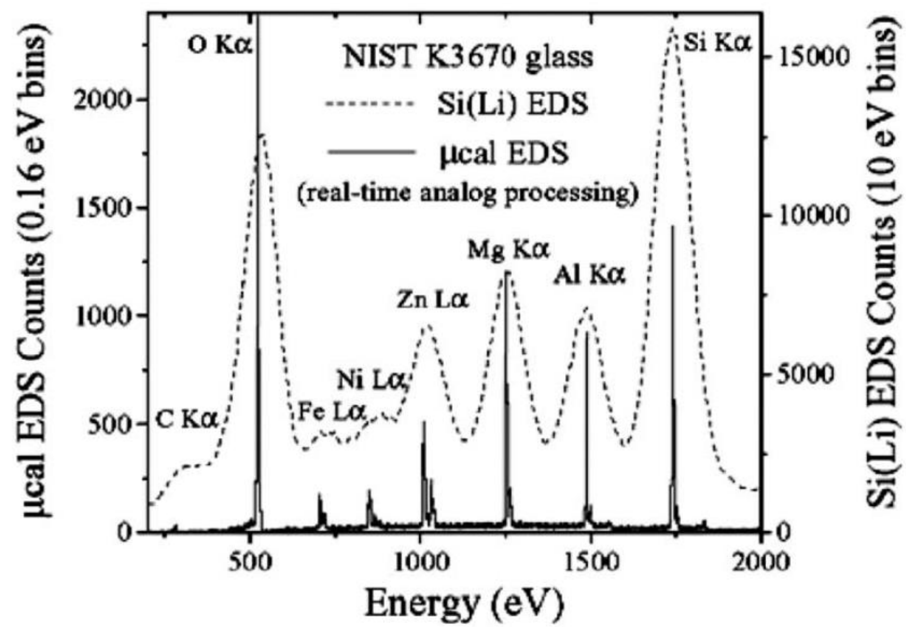

Energy resolution of the microcalorimeter, compared with a lithium drifted silicon detector.

Outline

- BNL Instrumentation Division
  - Facilities, accomplishments
- Detector and Electronics Trends (with selected examples)
  - Improved time resolution
    - Silicon detectors with avalanche gain
    - Wideband electronics
  - Improved spatial resolution
    - Fine-pitch pixels
    - Interpolation techniques
  - Improved energy resolution
    - Si detectors with low collection capacitance
    - Monolithic integration of sensors and electronics
    - Repetitive non-destructive readout
    - Cryogenic devices
- Highly-scaled systems
  - Inhospitable environments
    - Cryo
    - Vacuum
    - Radiation
  - Power and data bandwidth constraints

Approaches towards finer pitch pixel sensors, dissimilar technologies

Hybrid bump-bonding of sensor to ASIC

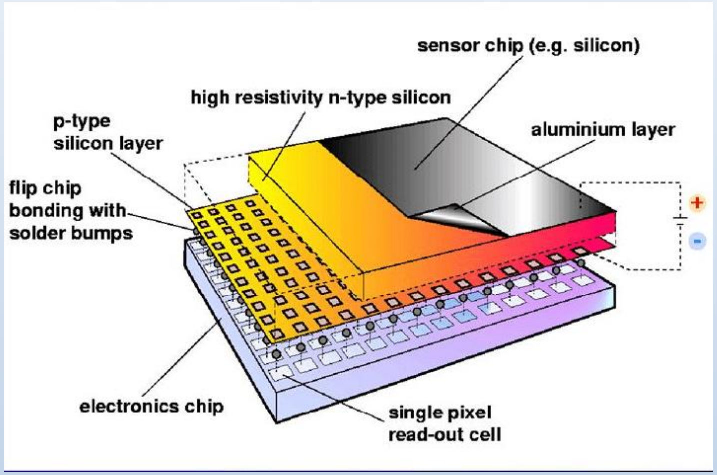

"2.5D" hybrid using glass or Si interposer

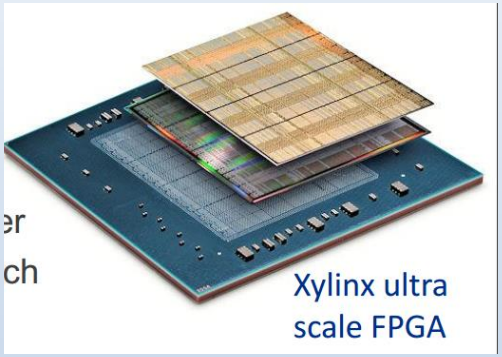

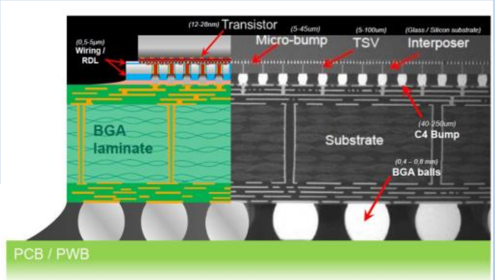

"3D" hybrid: direct wafer bond, multiple CMOS layers possible

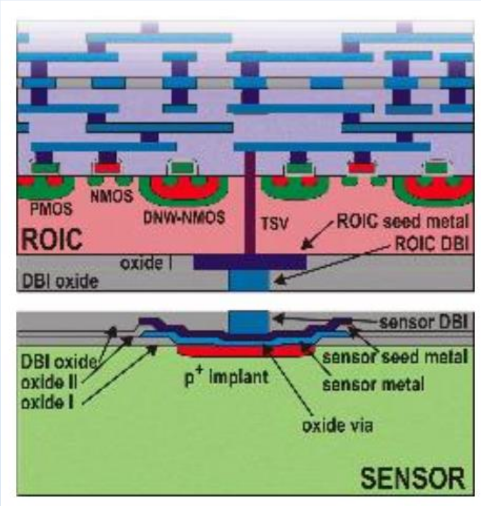

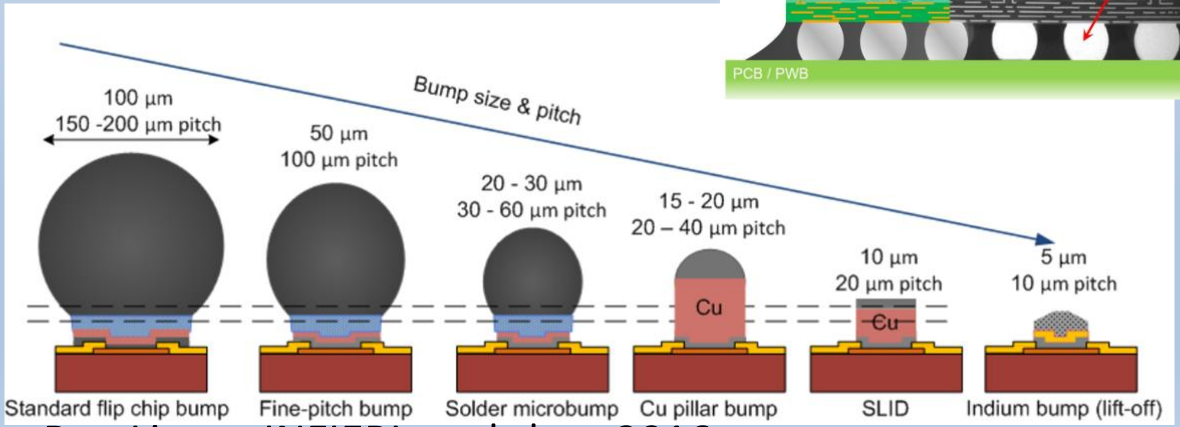

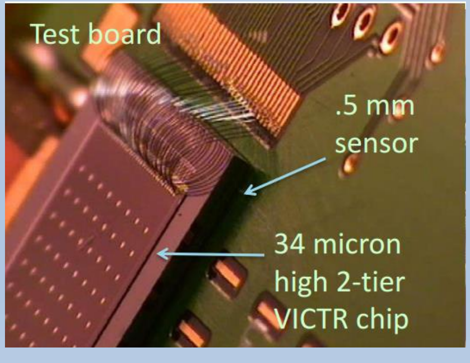

Ron Lipton INFIERI workshop 2016

Anode pad readout for ^{3}He Ionization mode neutron detector

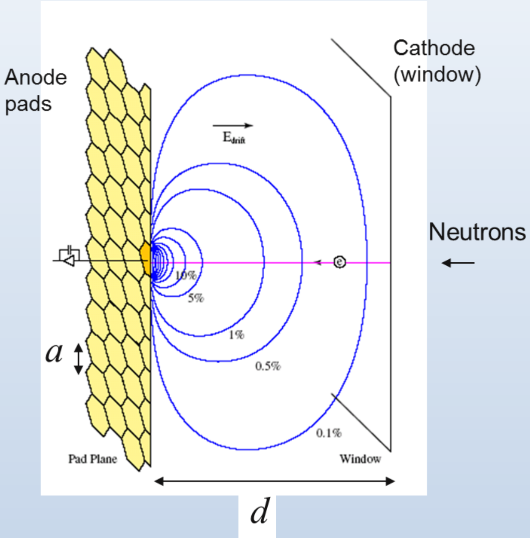

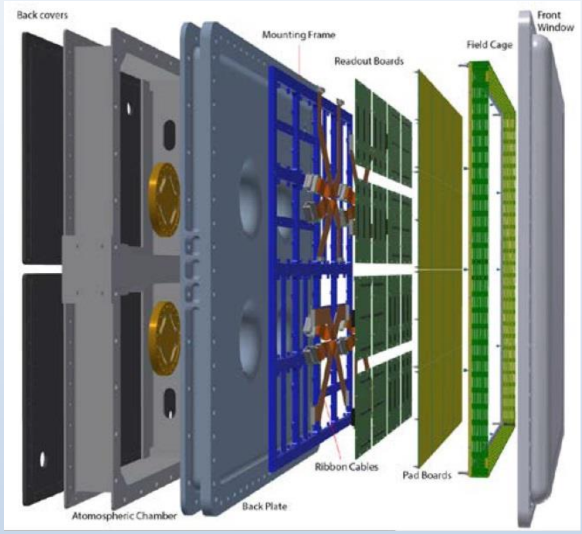

With low noise electronics, 5fC detectable with untiy gas gain. Pixelated anode plane only achievable with ASICs

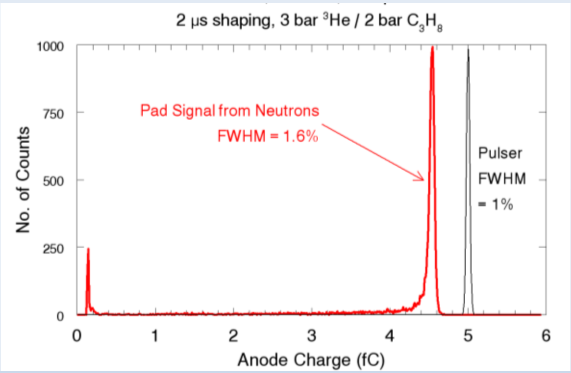

First image using Cd mask (BNL) and 1mCi ^{252}Cf source 22.5M hits

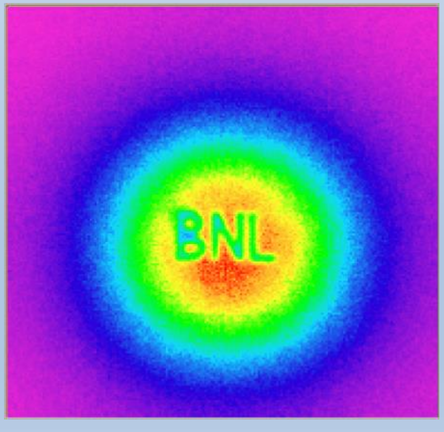

Neutron pad board front/back with ASICs

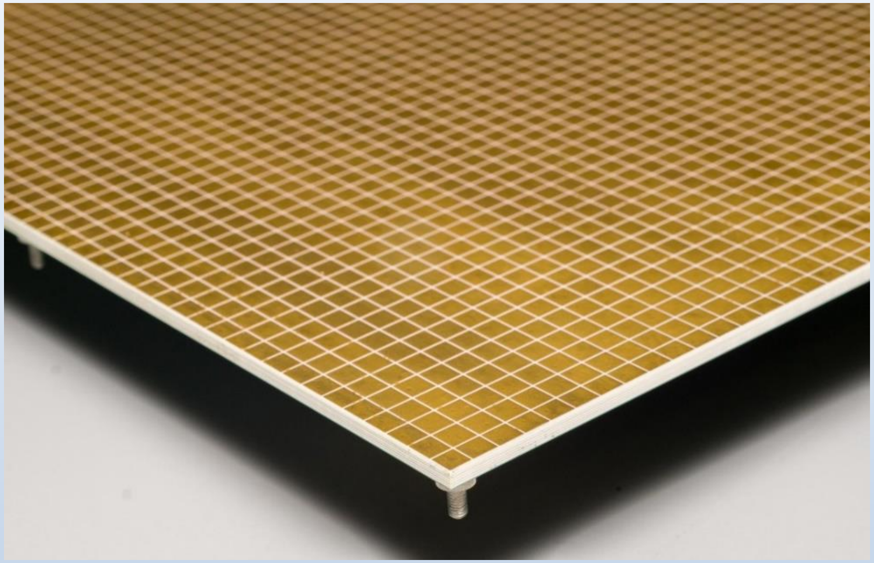

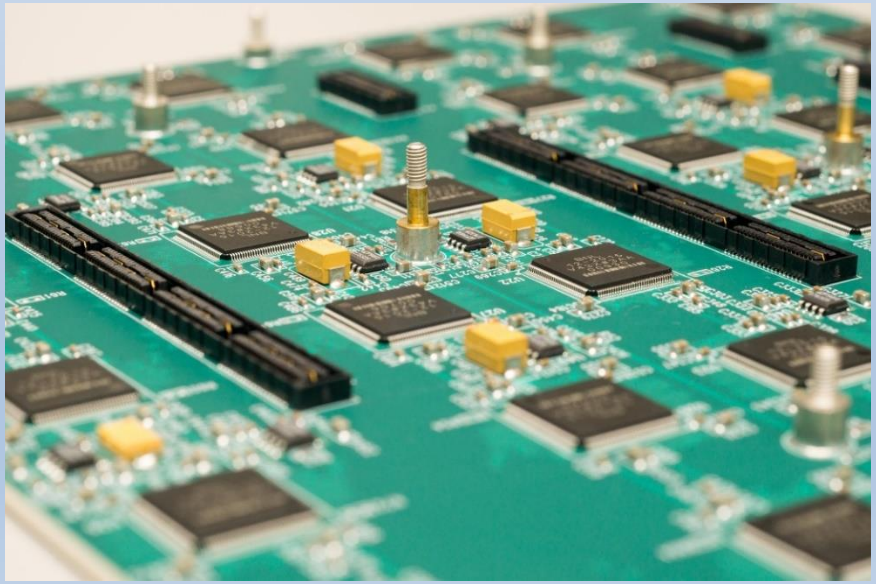

64-channel ASIC
All-digital output of charge/time/channel

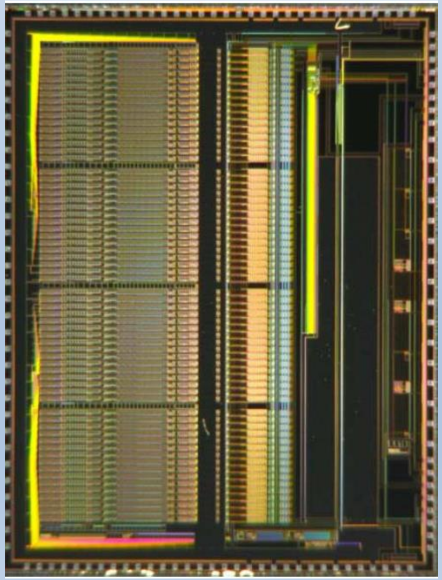

^{3}He pad detector - output data format

List mode data generated for each ionizing event

Book1 - Microsoft Excel

File Home Insert Page Layout Formulas Data Review View Acrobat

A1 *fx*

	A	B	C	D	E	F	G	H	I
1		Timing	Peak detect	Channel #	Chip #	Board #			
2	168	70623	12	34	27	15			
3	168	70620	8	35	27	15		34	
4	168	70625	9	38	27	15			
5	168	70624	5	39	27	15			
6	20	195008	10	46	0	9			
7	20	195006	5	46	10	9		36	
8	20	195008	9	51	0	9			
9	20	195006	11	17	11	9			
10	27	139023	7	42	34	1			
11	27	139026	9	45	34	1		37	
12	27	139023	5	50	34	1			
13	27	139027	15	55	34	1			
14	139	21652	12	14	16	7			
15	139	21656	7	50	15	7		37	
16	139	21652	8	9	16	7			
17	139	21652	10	13	16	7			
18	20	204339	15	52	35	10			
19	20	204336	6	53	35	10		39	
20	20	204342	10	56	35	10			
21	20	204336	8	57	35	10			
22	200	255288	8	58	32	7			
23	200	255290	14	59	32	7		40	
24	200	255291	10	60	32	7			
25	200	255295	8	35	32	7			
26	234	93852	6	31	33	4			
27	234	93852	6	3	33	4		31	
28	234	93854	6	4	33	4			
29	234	93854	13	27	33	4			

Sum of peaks in column C

Hits identified by time coincidence and adjacency

- New generation of ^{3}He –based, pixel ionization chambers (***unity gas gain***), enabled by microelectronics, makes possible ***high count rate capability, 10^5 /s per pixel, >10^8 /s per detector***, flexible geometry, absence of ageing effects, extraordinary stability and reliability, the narrowest neutron signal peak.
- The technology provides powerful discrimination, n/γ by pulse height, and n/particles by magnitude of charge and # of pads generating simultaneous signal.
- Time stamp applied to each signal provides TPC like operation – 3D rendition of events and tracks
- Systems can be fabricated in which front-end and DAQ are contained within the detector vessel, with only Gbit ethernet to a PC and power cables the only outside items.

Fast single-photon imager

CERN pixel chip “Timepix” hybridized to Si pixel sensor
Image intensifier for single-photon sensitivity
~10ns timing/20um position for single photons (1.5ns version in development)
Applications:
- Fluorescence decay chemical analysis
- Quantum communications (detect entangled photons)

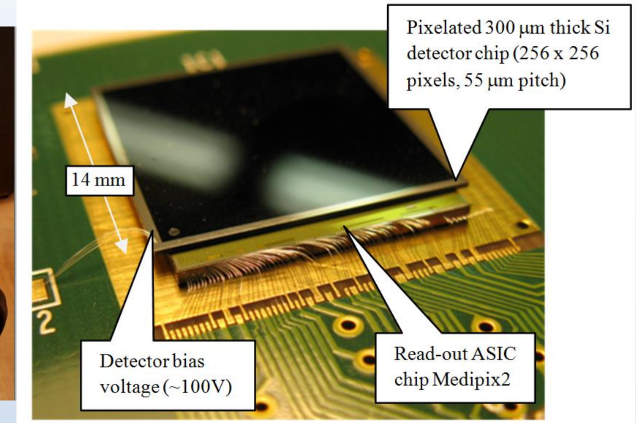

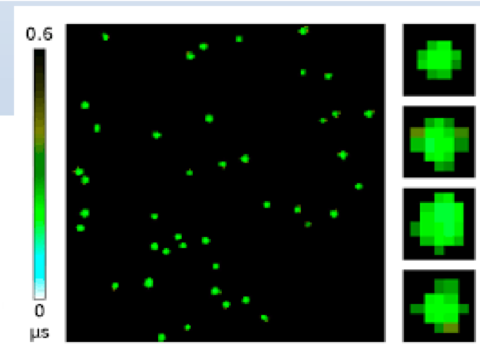

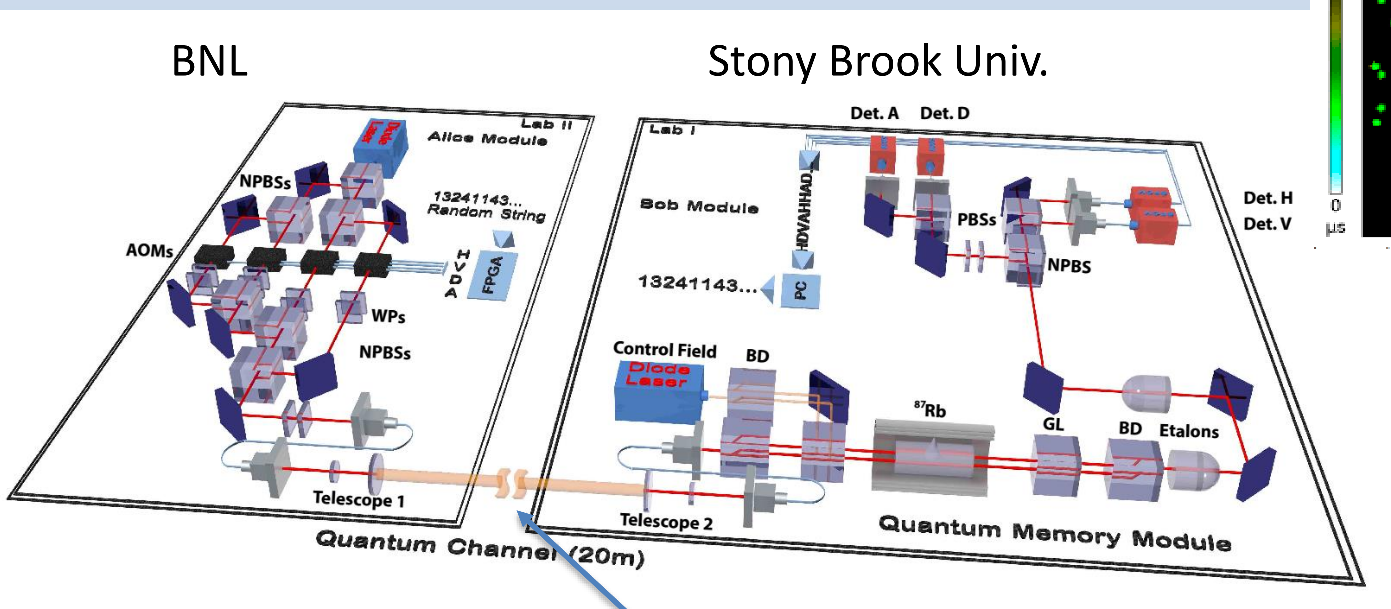

Free-space link

Multisite event reconstruction in CZT

- CdZnTe (CZT) room temperature semiconductor gamma ray detector produced up to ~2cm thickness
- Has significant material nonuniformities
- Can be corrected by 3D calibration of entire detector “cube”
- Compton events contained within crystal (or crystal array) can be reconstructed
- Compton kinematics allows source localization (Compton telescope)

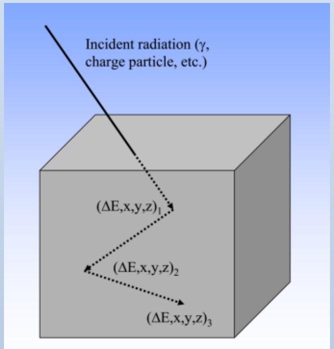

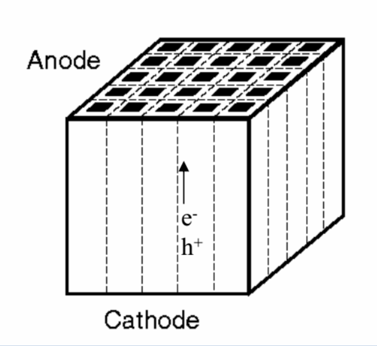

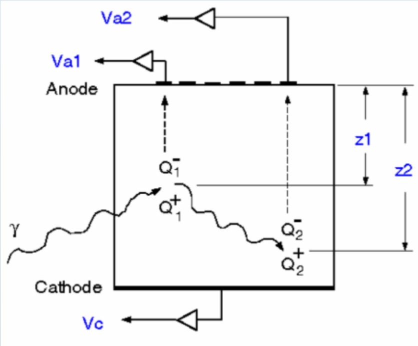

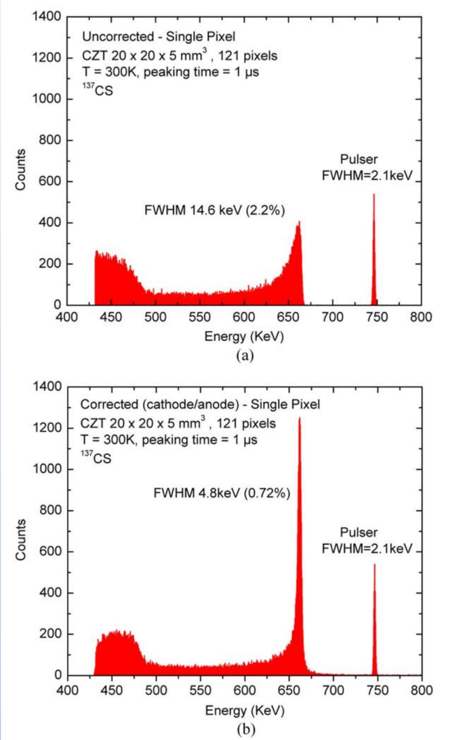

Fig. 16. Single pixel spectrum from a ^{137}Cs source: (a) uncorrected, and (b) corrected using the cathode/anode ratio.

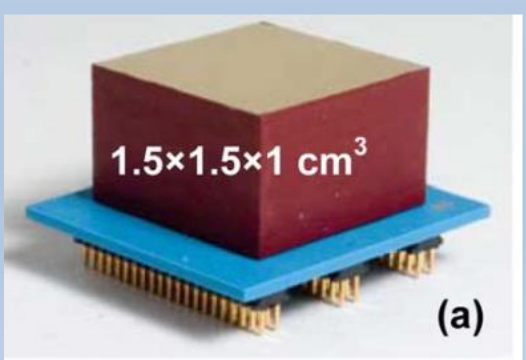

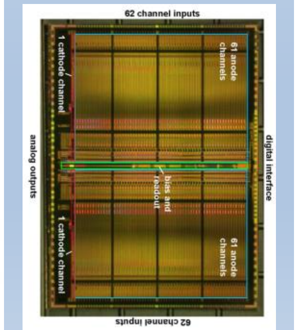

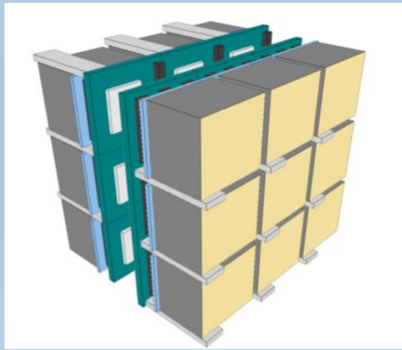

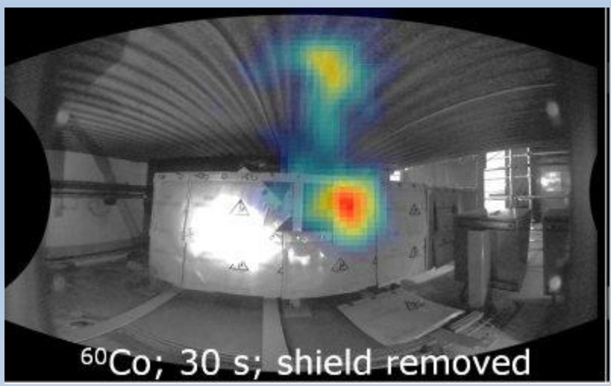

Outline

- BNL Instrumentation Division
  - Facilities, accomplishments
- Detector and Electronics Trends (with selected examples)
  - Improved time resolution
    - Silicon detectors with avalanche gain
    - Wideband electronics
  - Improved spatial resolution
    - Fine-pitch pixels
    - Interpolation techniques
  - Improved energy resolution
    - Si detectors with low collection capacitance
    - Monolithic integration of sensors and electronics
    - Repetitive non-destructive readout
    - Cryogenic devices
- **Highly-scaled systems**
  - **Inhospitable environments**
    - Cryo
    - Vacuum
    - Radiation
  - **Power and data bandwidth constraints**

Detectors getting larger over time

Silicon tracking @ colliders

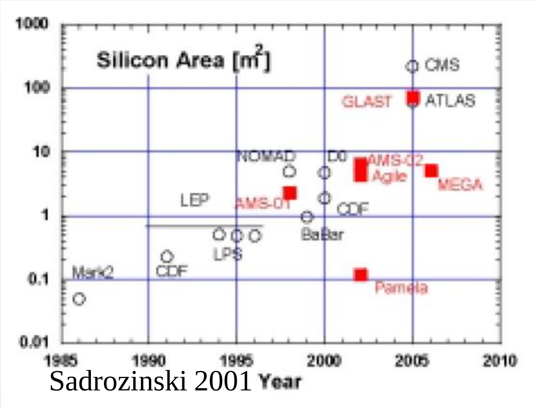

Astronomical mosaic cameras

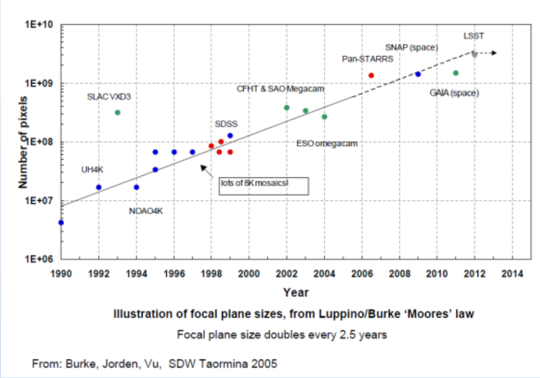

CMB

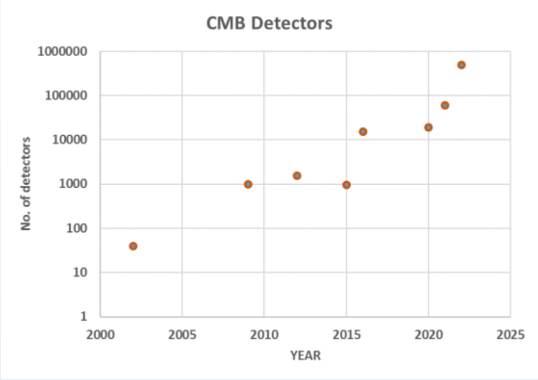

LAr TPCs

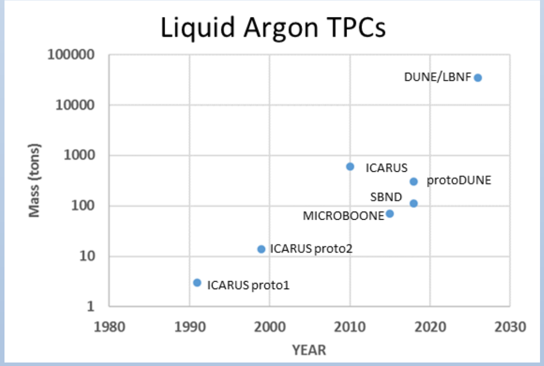

21cm radio arrays

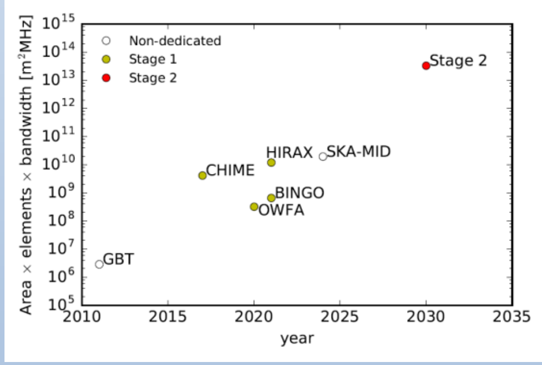

Computing needs

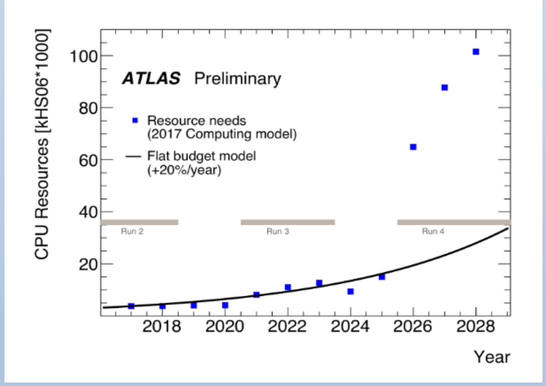

Detector services (***power***, cooling, data I/O) consuming a larger share of R&D and construction effort

Importance of power planning

- Electronic circuits are usually regarded as manipulators of signals and information
- Frequently neglected is that they are also thermodynamic machines and the electrical manipulations incur a cost in power dissipation

Awareness of power tradeoffs is needed at the transistor/technology, circuit, and system level:

- *Many performance parameters have a steep dependence on expended power*
- *For large, highly integrated systems it is easy to underestimate the engineering challenges of managing power delivery and heat removal*

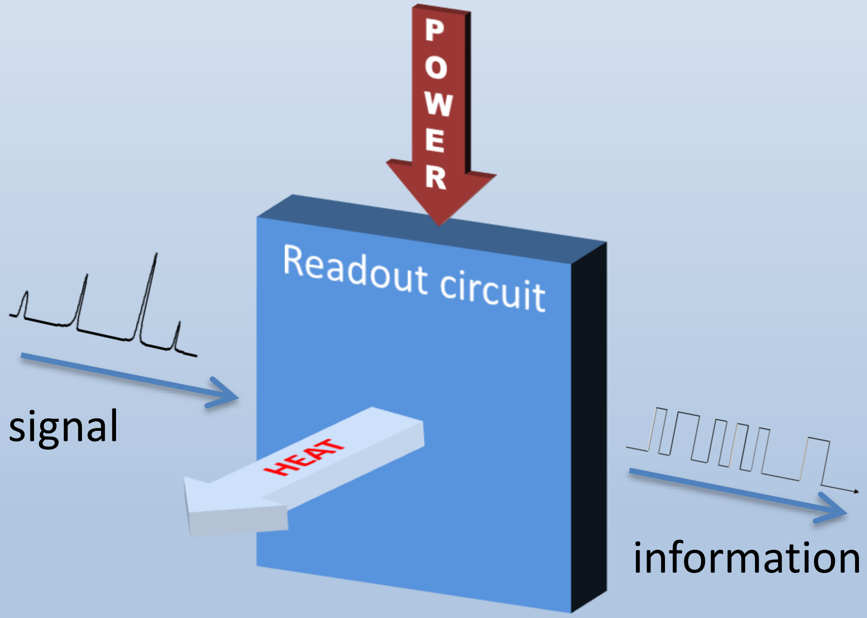

Is there more efficient way to extract the information in the signal?

Conventional signal chain

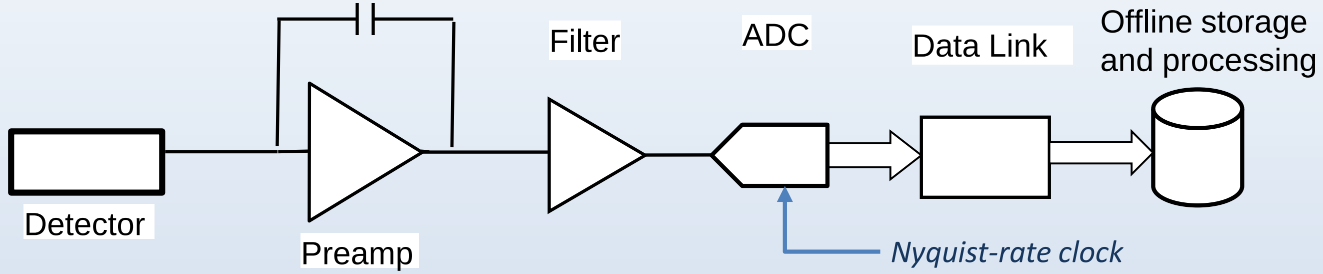

Raw: 15MB | JPEG: 150KB

One can regard the possibility of digital compression as a failure of sensor design.
If it is possible to compress measured data, one might argue that ***too many measurements were taken***
-- David Brady

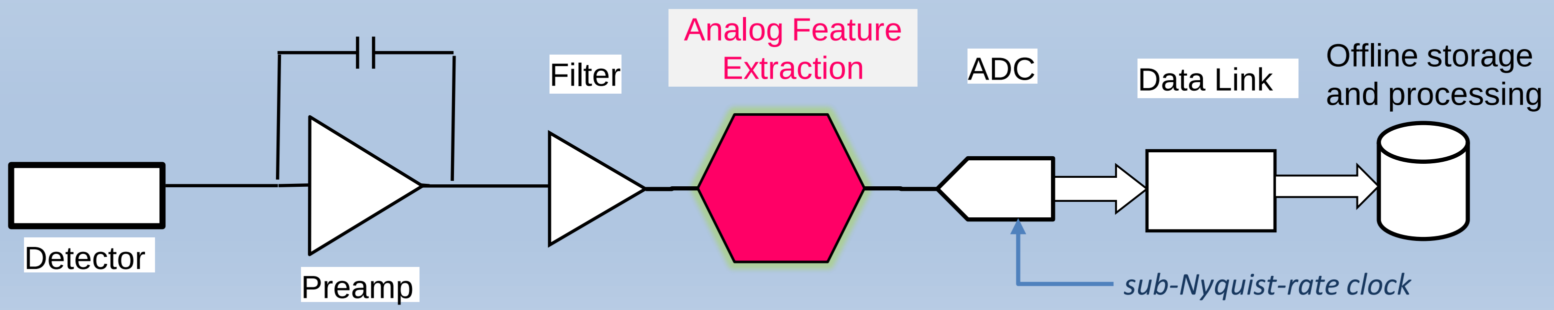

Outlook

- Dramatic recent progress in energy-resolving (RNDR, TES) and time-resolving (SPAD, LGAD) opening new experimental opportunities
- Technology advances permitting ever-finer detector granularity, and closer integration of sensor and front-end electronics
  - Fine-pitch bump bonding, 3D integration of Si and readout ASIC
  - Microwave multiplexing enabling large TES arrays
  - Power dissipation / power density constraints increasingly being realized
- Opportunities for borrowing power-efficiency techniques from commercial world
  - Conditional powering, activity detection
  - Analog feature extraction
  - Machine learning/deep learning
  - Compressive sensing
- Larger projects / larger budgets brining sociological change to experimental groups
- New focus area of quantum sensing receiving attention

Hope to see you at BNL next Wednesday!

Microprocessor speed and power trend

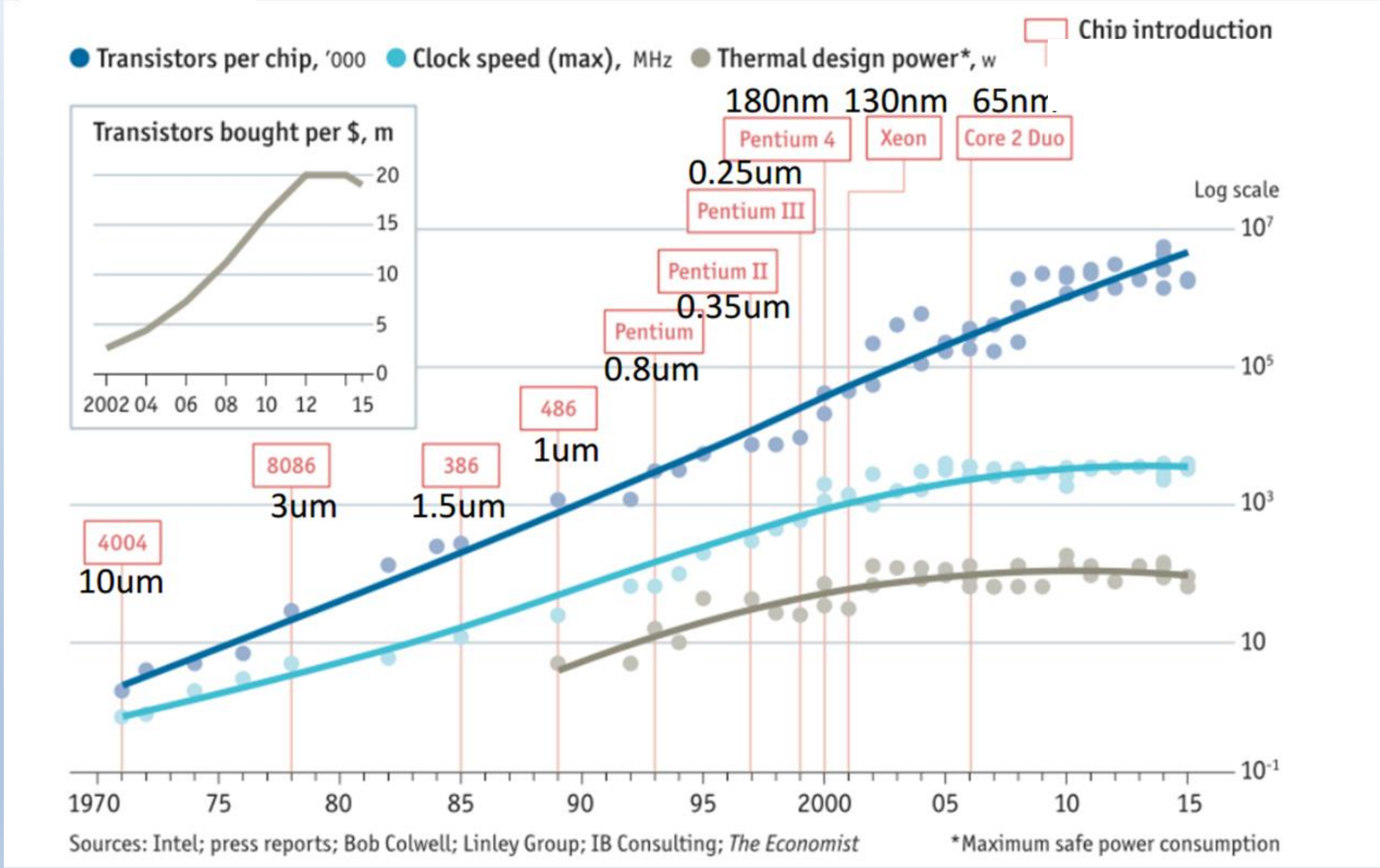

Cray-2 supercomputer (1985)

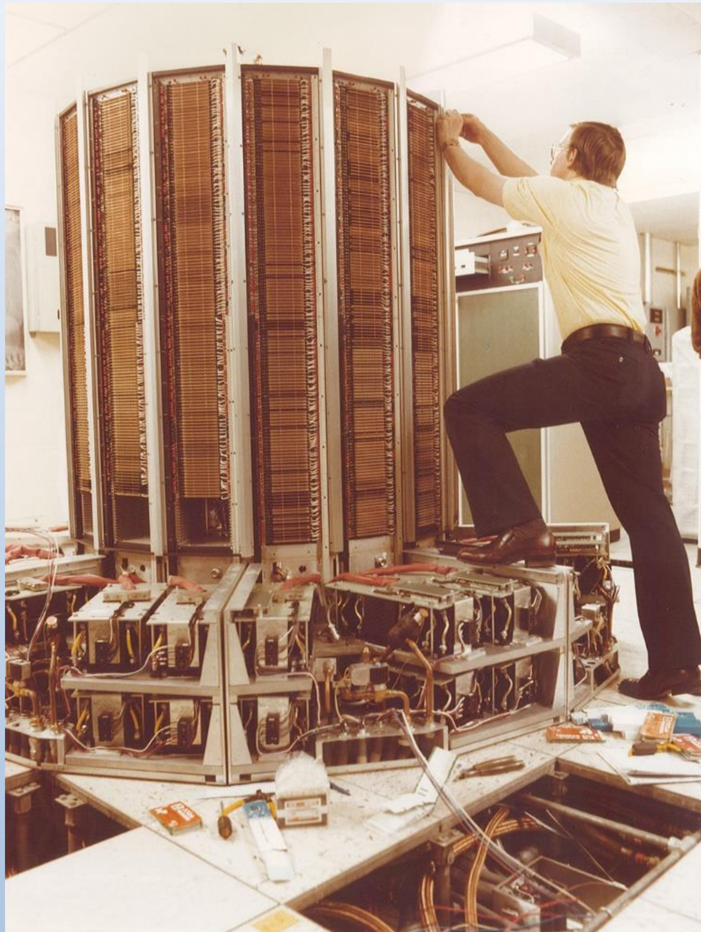

- 4 processors
- 1.9 GFLOPS peak
- Clock speed 0.25GHz
- 2500kg
- 200kW

Logic module

Transistor power vs. speed and noise

- In analog CMOS, designer selects technology feature size, transistor geometry (gate length and width), transistor polarity (NMOS/PMOS), and bias current
- Current density (I/W) determines state of inversion (weak/moderate/strong)
- In deep submicron technologies, weak/moderate inversion is typical bias condition

Power vs. cutoff frequency

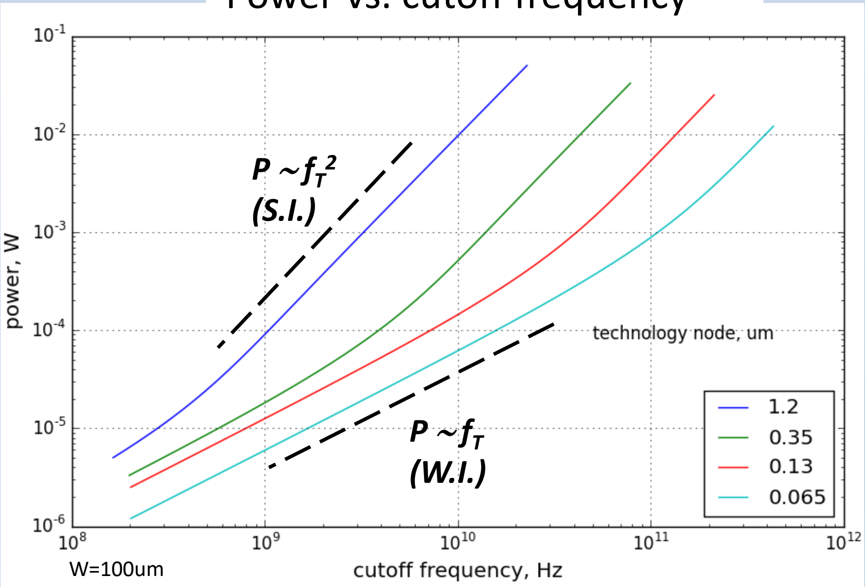

Power vs. input noise density

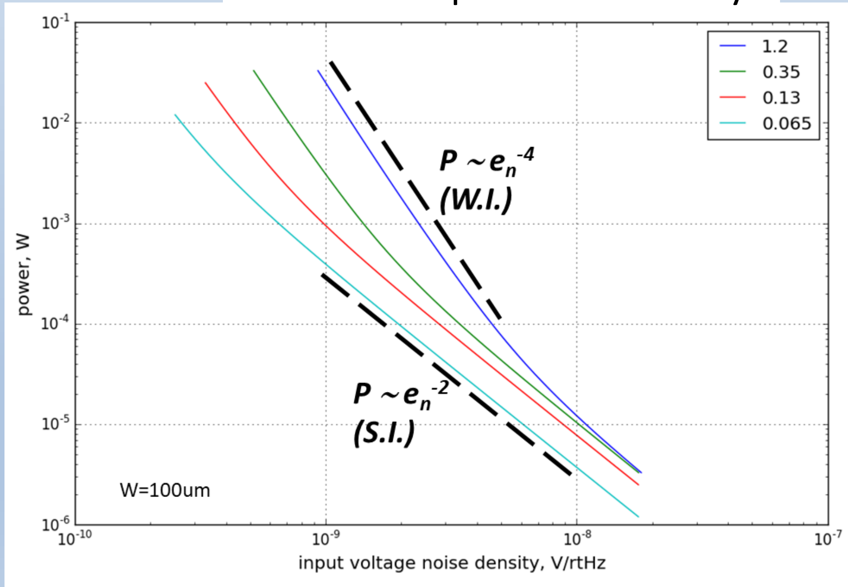

Analog-to-digital conversion energy

- Figure-of-merit for AD converters (energy per conversion): $FOM = \frac{P_{diss}}{f_s}$
- Thermal limit: $\frac{P}{f_s} \geq 4 \cdot kT \cdot SNR$

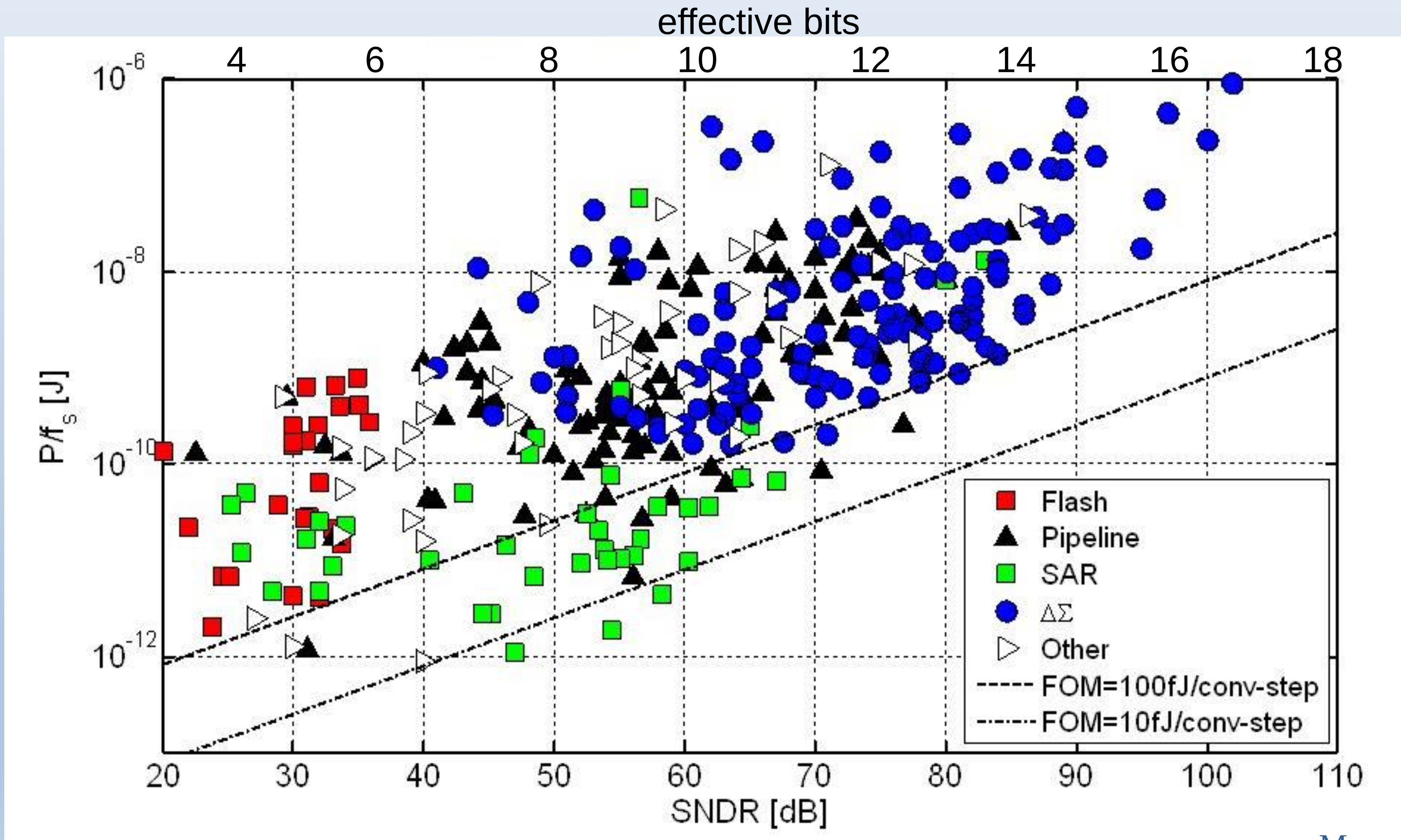

Murmann 2008

Digital data link power

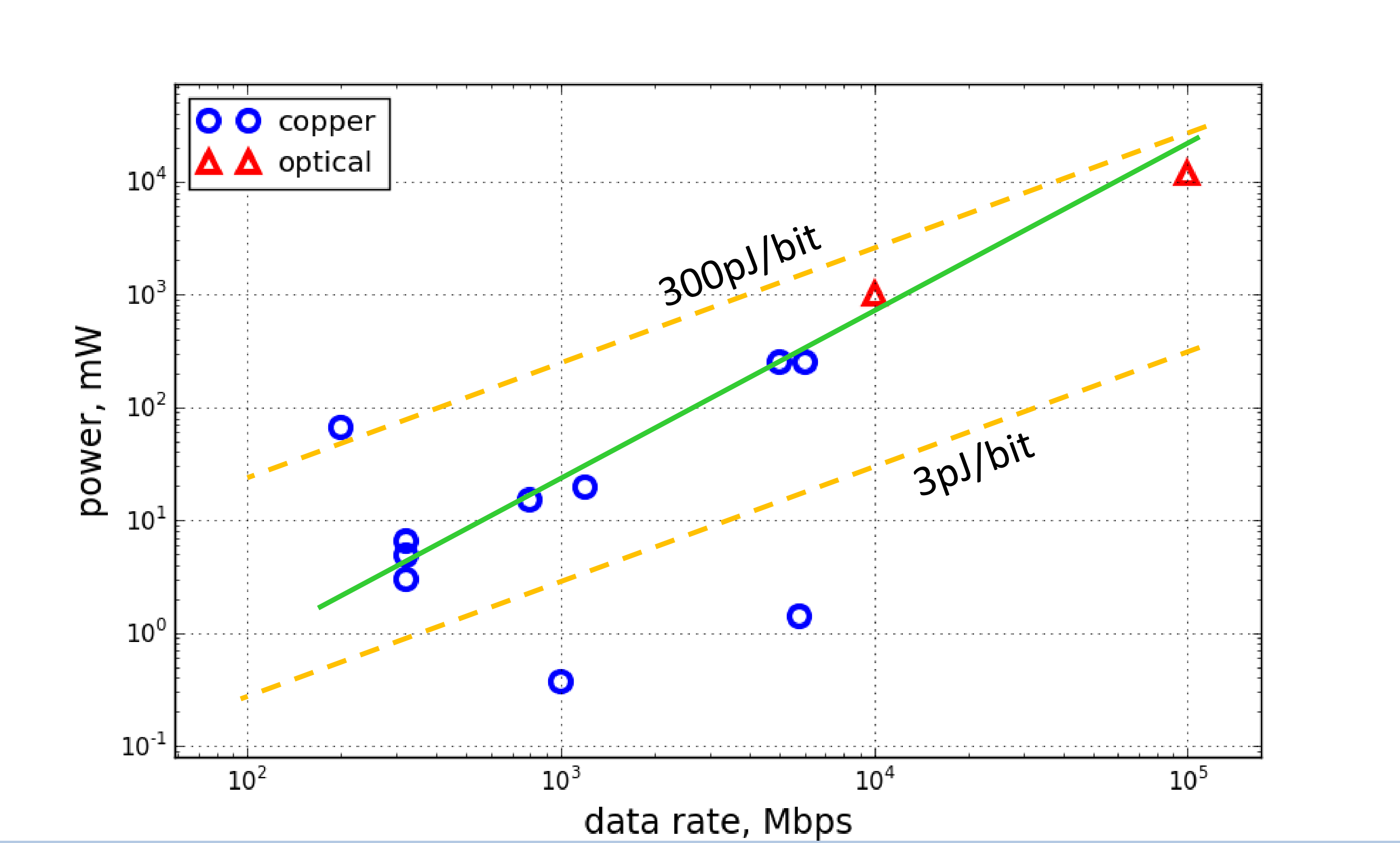

Digitally-assisted analog

- in 90nm CMOS, more than 2,000,000 gates would need to switch to consume the energy an A/D conversion at 16b resolution
- It pays to take advantage of the availability of abundant digital resources to enhance the performance and precision of analog circuits
  - Mismatch correction
  - Nonlinearity correction
  - Correction of dynamic errors allowing the use of "mimimalistic" analog topologies

Single-transistor residue amplifier

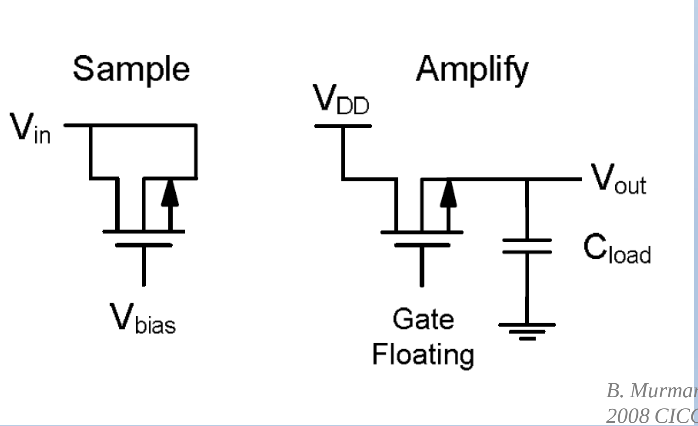

B. Murmann, "A/D Converter Trends: Power dissipation, scaling and digitally assisted architectures", IEEE 2008 CICC 7-5-1
J. Hu et al., "a 9.4bit, 50MS/s, 1.44mW pipelined ADC using dynamic residue amplification", Dig. VLSI Circuits Symposium, Jun. 2008

Measurement of step height (CCD)

Dual-slope integrator (differential averager) is the matched filter for step waveform with white noise
As long as the pixel frequency is greater than the 1/f noise corner, noise is within 5% of ideal

CCD signal

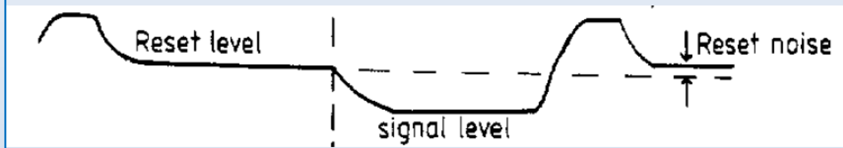

Optimal filter

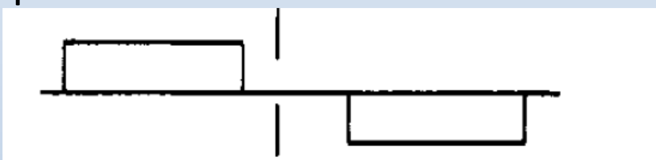

Digital CDS implementation

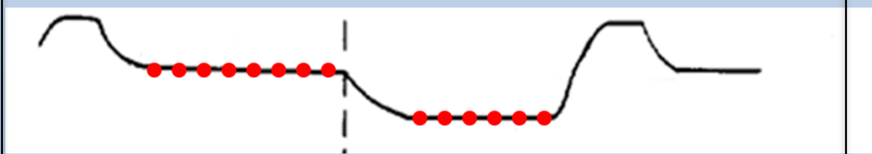

~20 samples/pixel

Total energy per pixel:
20 × 10.7nJ + 360b × 100pJ/bit = ***250nJ***

Analog dual-slope integrator

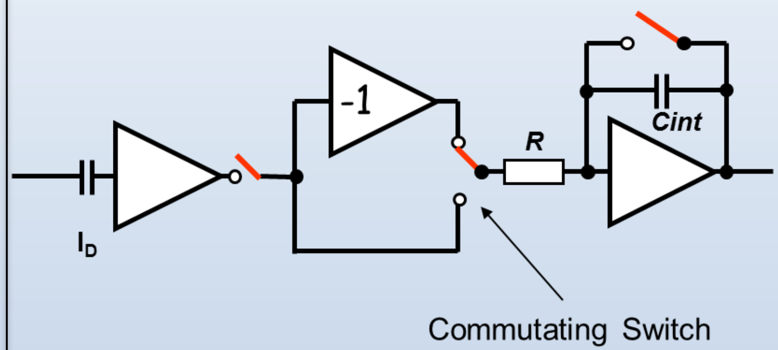

1 sample/pixel

Total energy per pixel:
35mW/560kHz + 1 × 10.7nJ + 18b × 100pJ/bit = ***75nJ***

CMOS peak detector

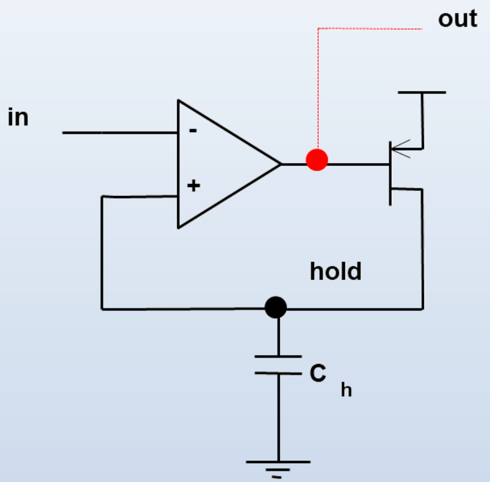

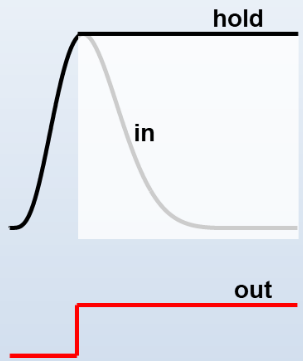

V_{out} is free of time-walk

Risetime

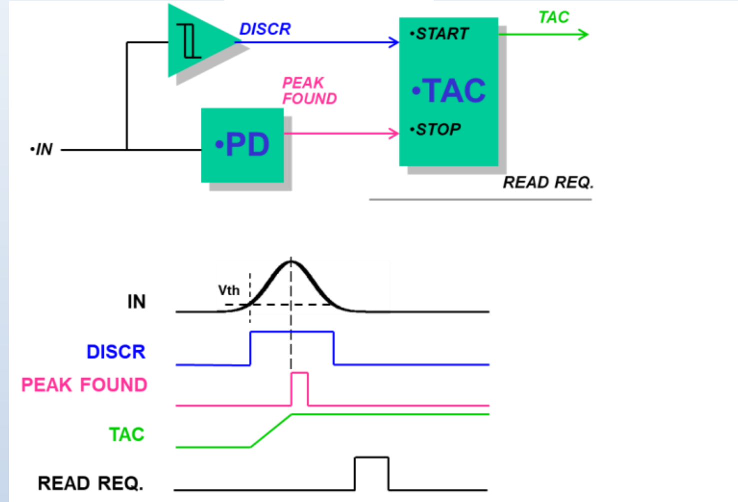

Time-over-threshold

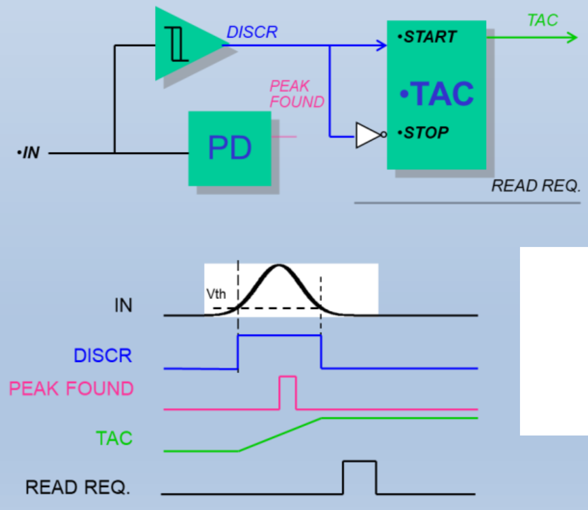

Time of occurrence

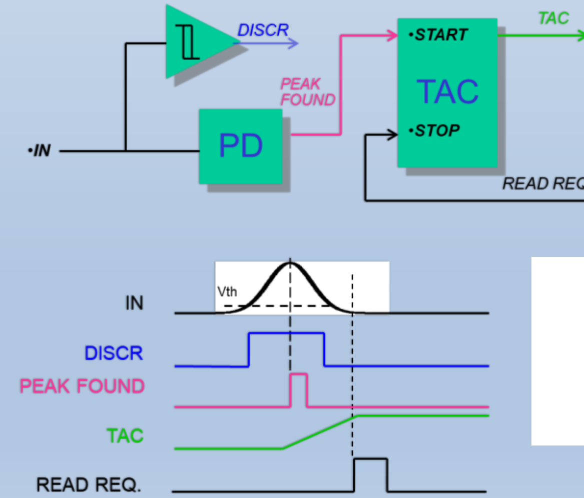

Multichannel system – sharing of peak detectors

Peak detector per channel

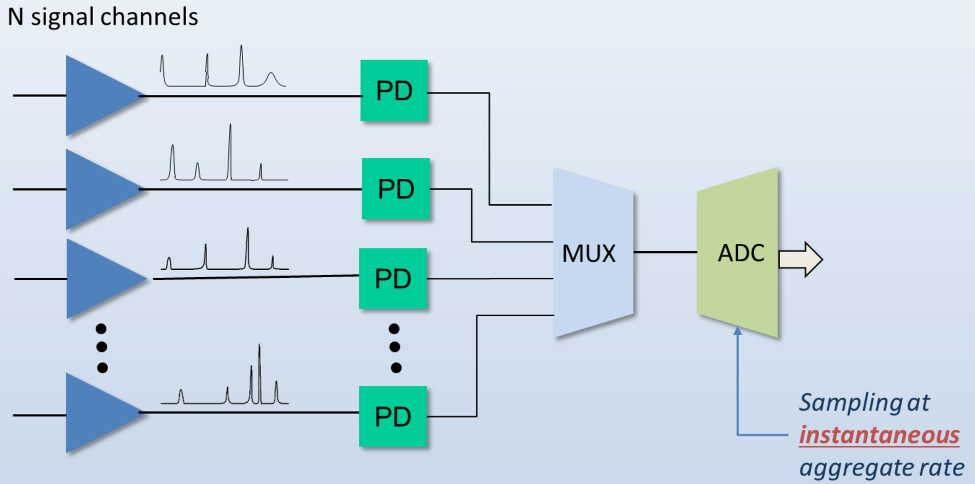

Shared peak detector bank with activity detection

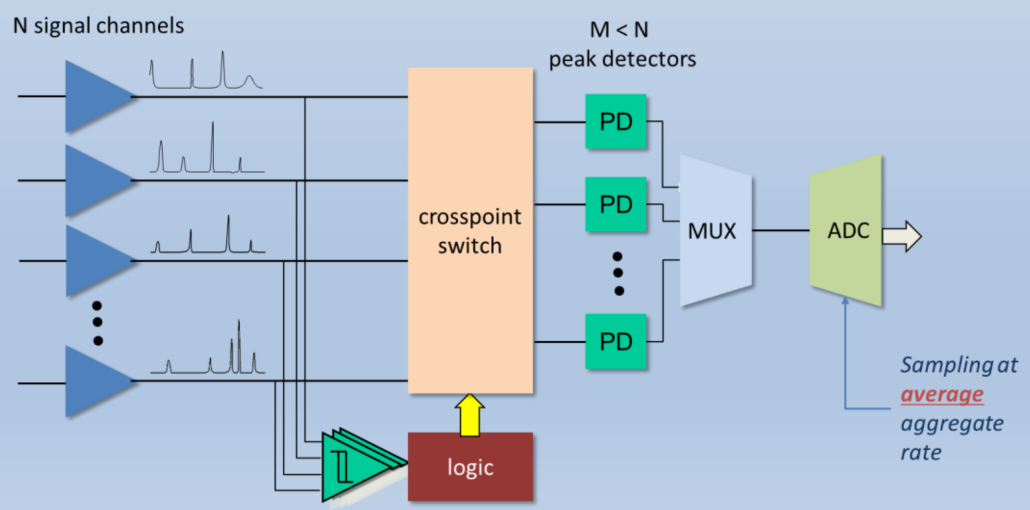

SCEPTER ASIC

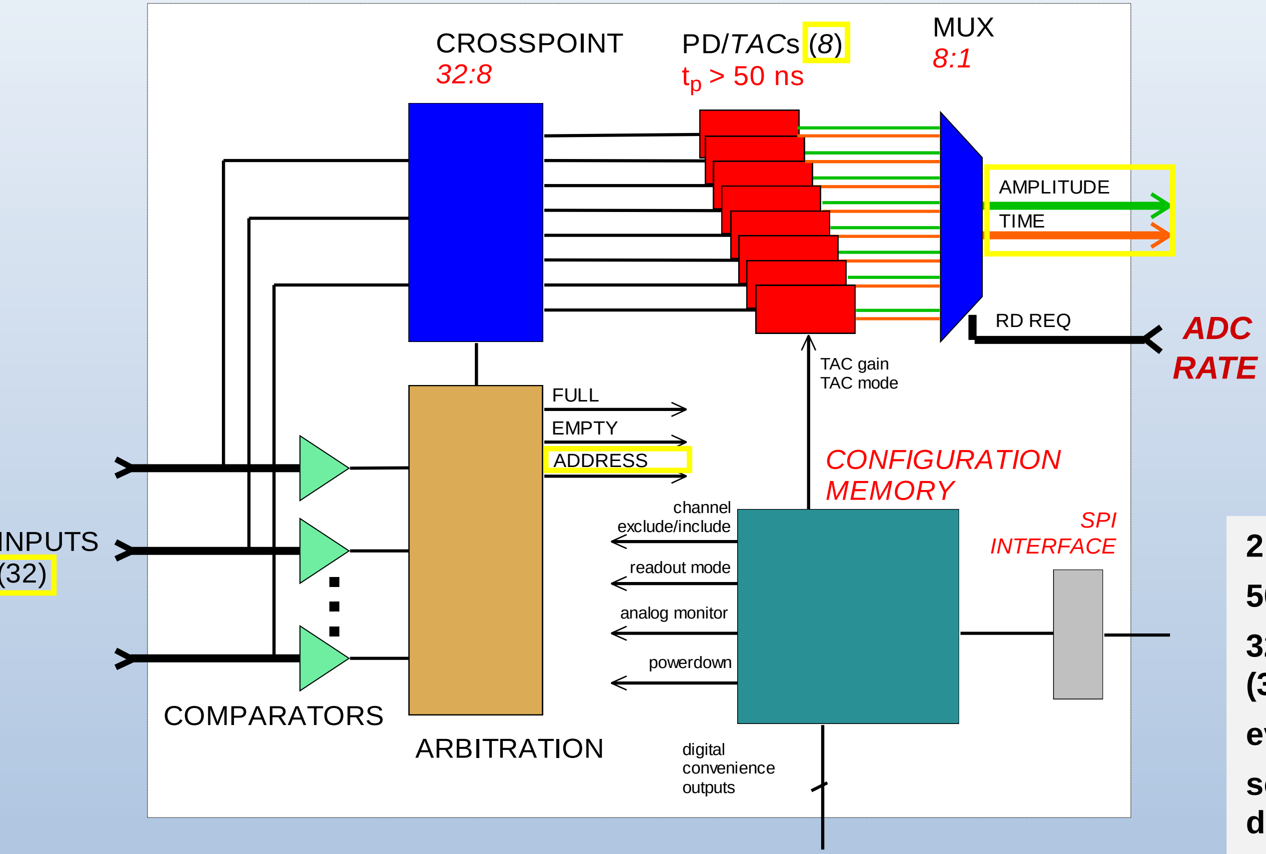

2 mW / channel

50 MS/s rate capability

32:1 multiplexing of shaped input signals (30ns peak time)

event amplitude, timing, address

self-triggering, sparsification, derandomization, data concentration

0.35um CMOS 3.3V

3.2 x 3.2 mm^2

P. O'Connor, G. De Geronimo, A. Kandasamy, IEEE Trans. Nucl. Sci. 50(4), pp. 892-897 (Aug. 2003).

Peak- and time-detector with analog derandomization

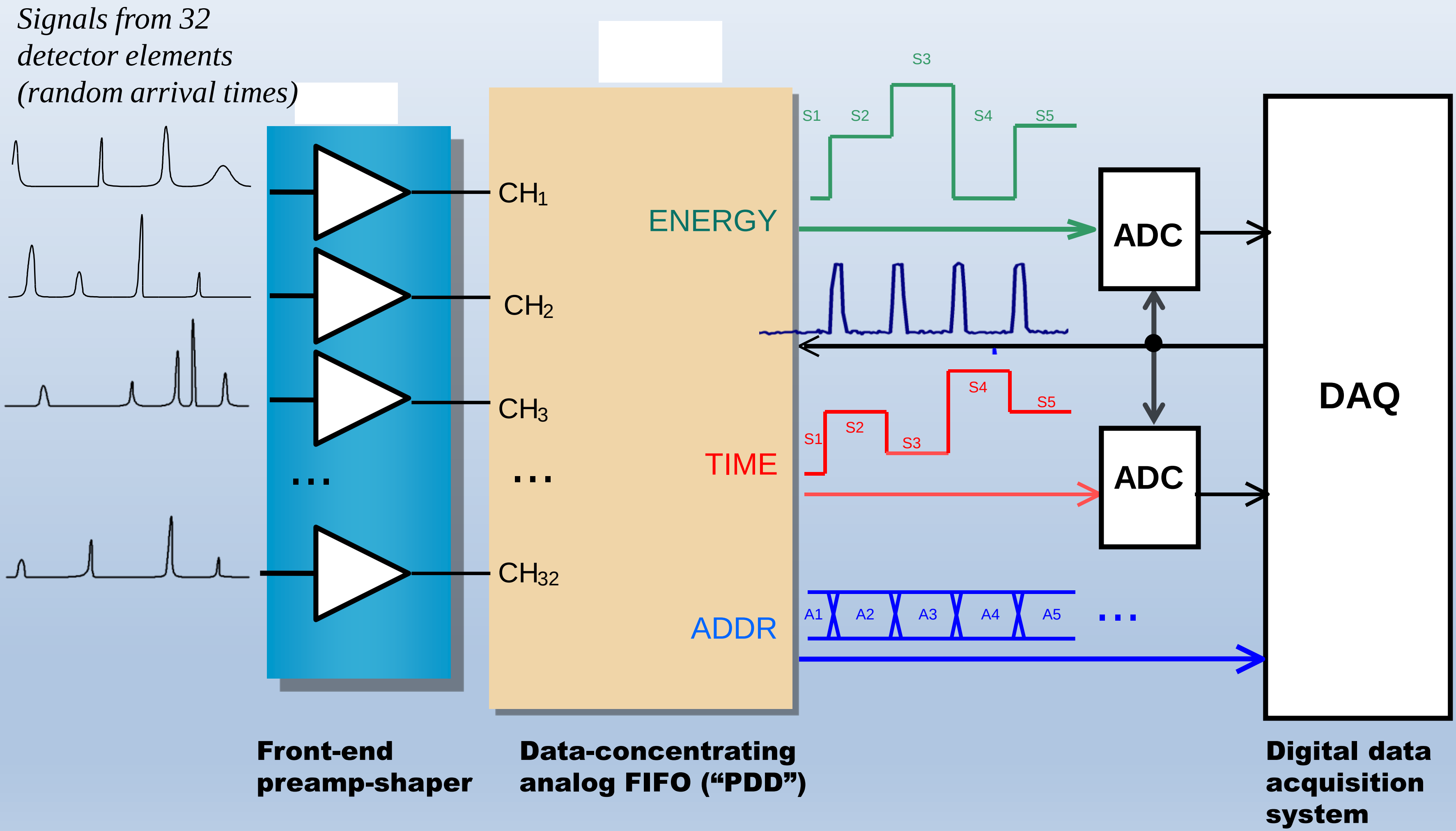

SCEPTER ASIC in MAIA Detector

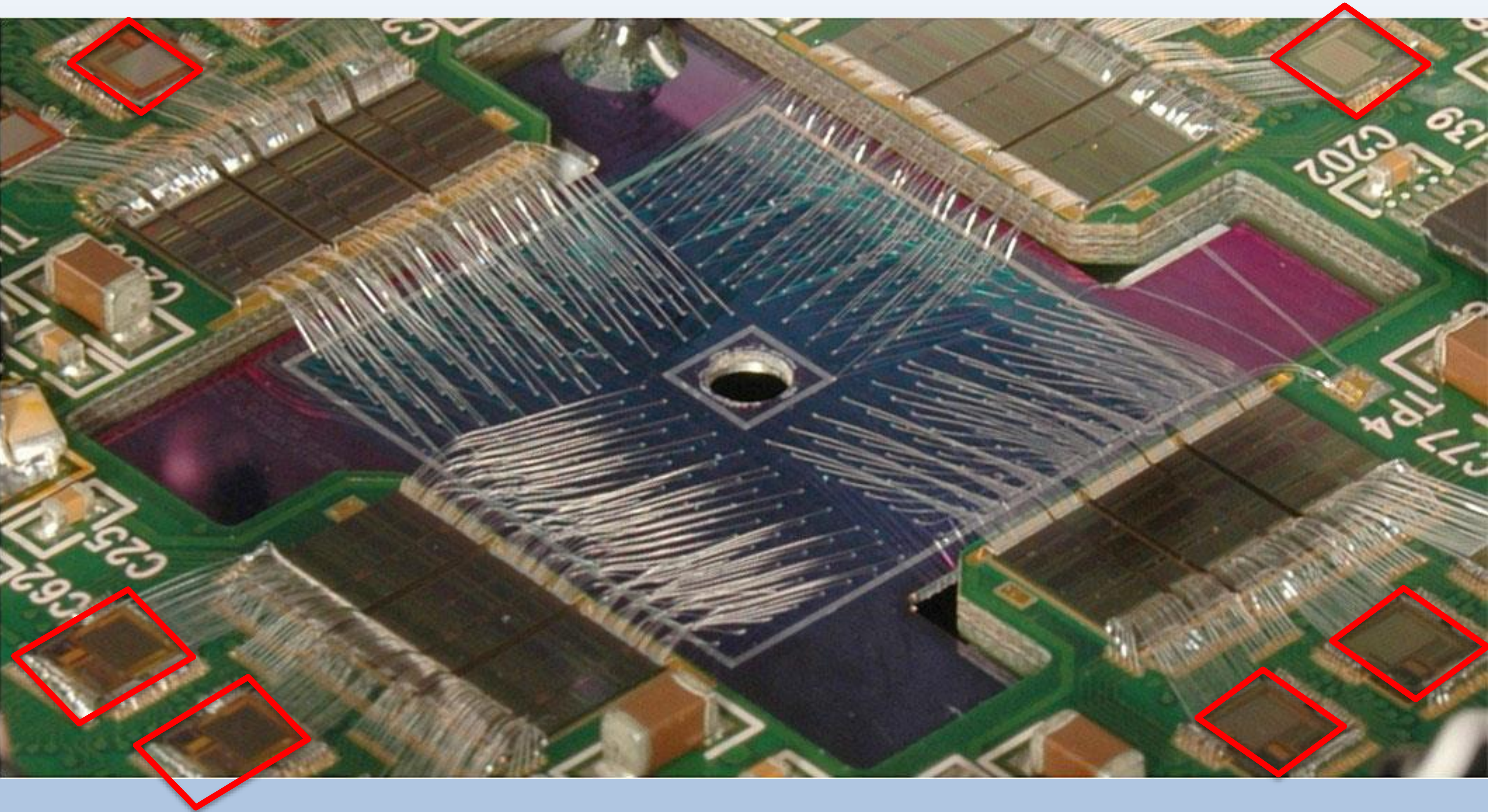

SCEPTER measurements

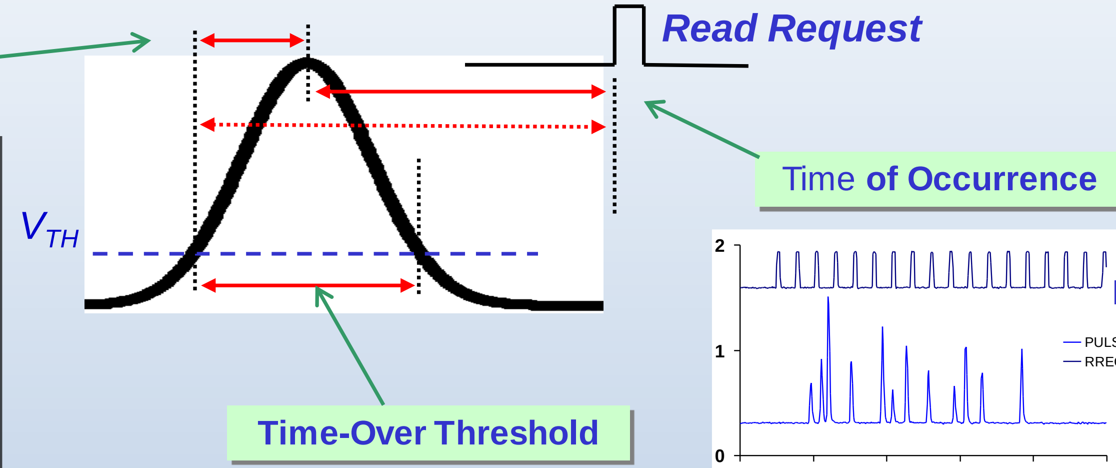

Sensor:

CZT pixelated linear array

32 elements, 16x3x3 mm^3

Rate:

~ 4.5 Mcps overall

~ 210 kcps single pixel

Resolution:

~ 3.4% (2.0keV) @ 60 keV

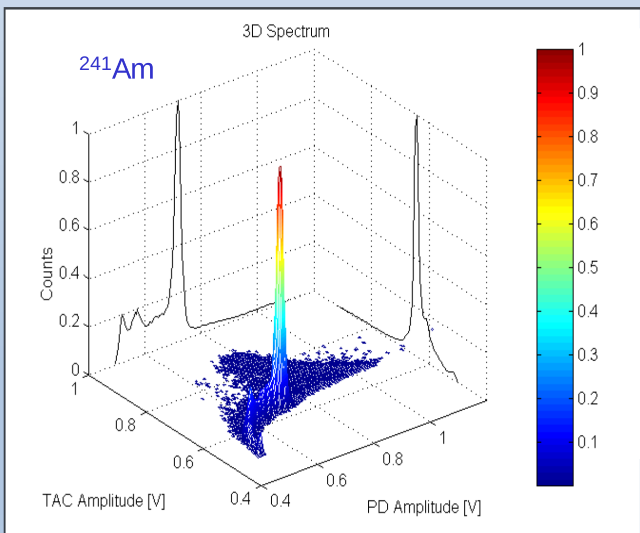

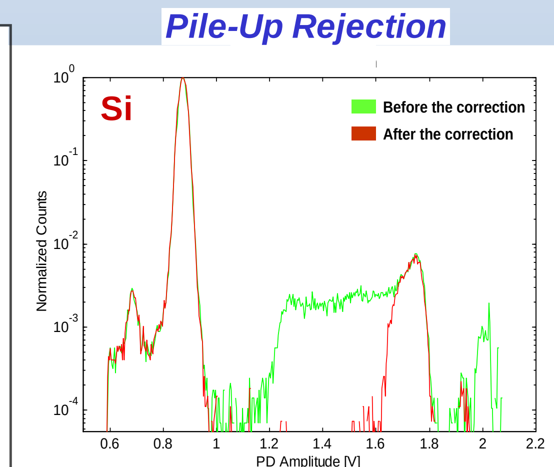

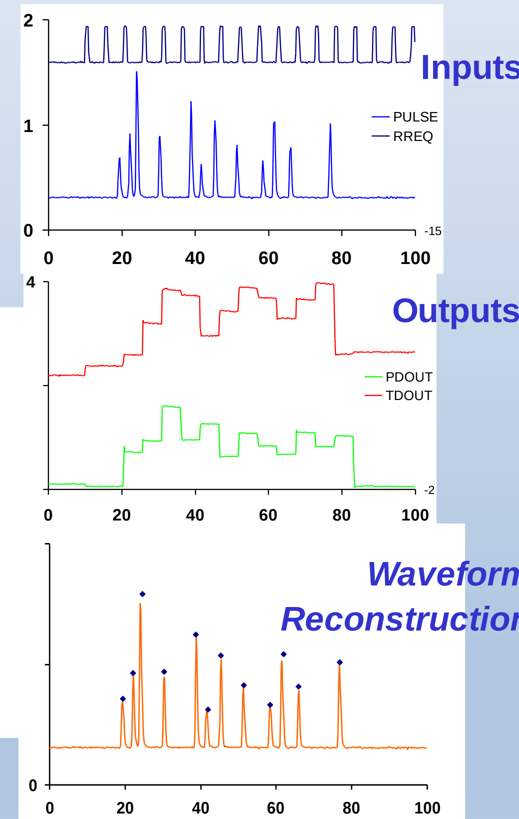

Dragone, A., De Geronimo, G., Fried, J., Kandasamy, A., O'Connor, P., Siddons, D. P., Corsi, F. (2006). Pile up rejection and multiple simultaneous events acquisition with the PDD ASIC. In Research in Microelectronics and Electronics 2006, Ph. D. (pp. 381-384). IEEE.

40 kTon LAr
DUNE (SP): 2 MHz sampling x
x 1536000 channels = 37 TB/s
For all data this is 145 EB/year

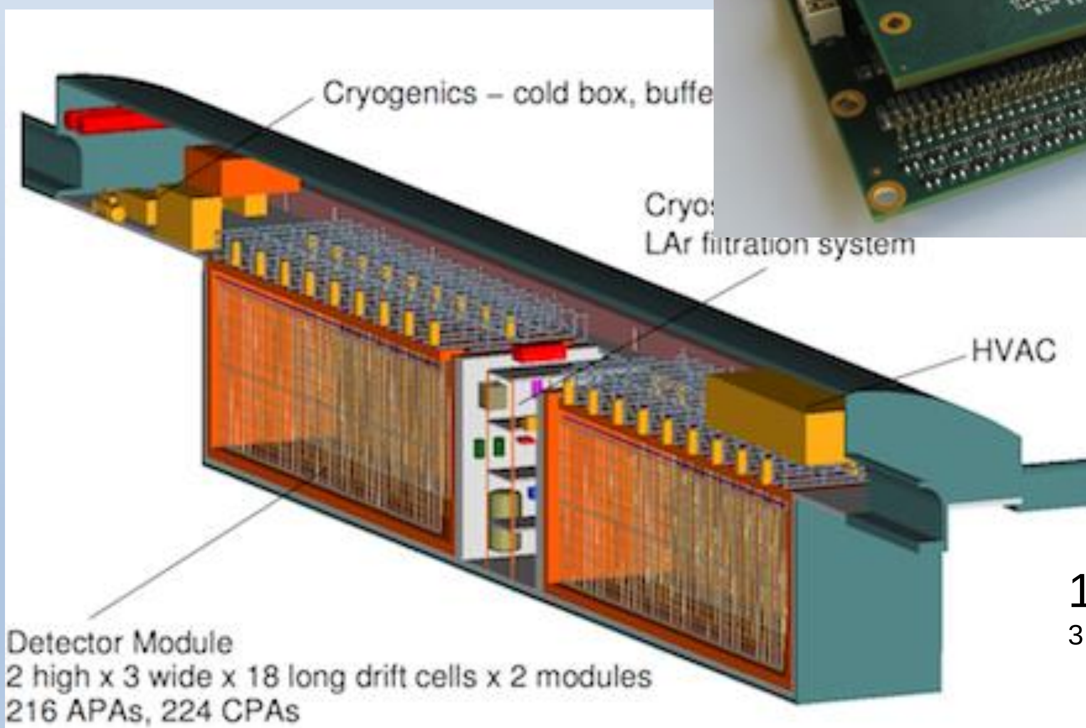

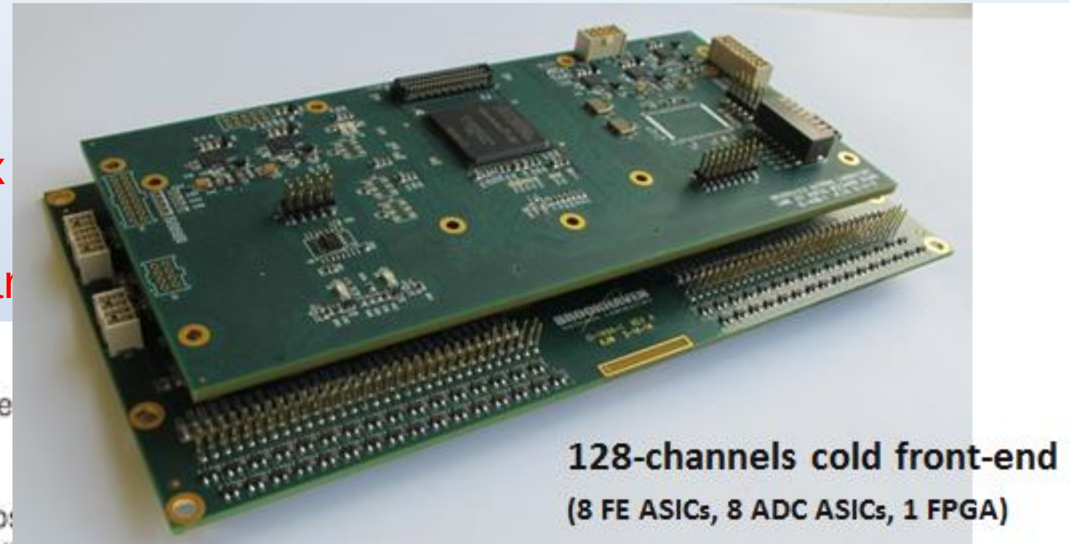

15.1 (W) x 14.0 (H) x 62 (L) m
3